Journal of Computational Mathematics
Vol.xx, No.x, 2023, 1–29.

http://www.global-sci.org/jcm
doi:10.4208/jcm.2302-m2022-0111

A FINITE DIFFERENCE METHOD FOR TWO DIMENSIONAL ELLIPTIC INTERFACE PROBLEMS WITH IMPERFECT CONTACT*

Fujun Cao[1)]
School of Science, Inner Mongolia University of Science and Technology, Baotou 014010, China
Email:caofujun@imust.edu.cn
Dongxu Jia
School of Science, Tianjin University of Technology, Tianjin 300384, China
Email:jiadongxu2012@mail.nankai.edu.cn
Dongfang Yuan
School of Science, Inner Mongolia University of Science and Technology, Baotou 014010, Inner Mongolia, China
Email: yuandf@imust.edu.cn
Guangwei Yuan[1)]
Laboratory of Computational Physics, Institute of Applied Physics and Computational Mathematics, P.O. Box 8009, Beijing 100088, China
Email: yuan_guangwei@iapcm.ac.cn

Abstract

In this paper two dimensional elliptic interface problem with imperfect contact is considered, which is featured by the implicit jump condition imposed on the imperfect contact interface, and the jumping quantity of the unknown is related to the flux across the interface. A finite difference method is constructed for the 2D elliptic interface problems with straight and curve interface shapes. Then, the stability and convergence analysis are given for the constructed scheme. Further, in particular case, it is proved to be monotone. Numerical examples for elliptic interface problems with straight and curve interface shapes are tested to verify the performance of the scheme. The numerical results demonstrate that it obtains approximately second-order accuracy for elliptic interface equations with implicit jump condition.

Mathematics subject classification: 65N06, 65B99.
Key words: Finite difference method, Elliptic interface problem, Imperfect contact.

1. Introduction

We consider the elliptic interface problem with imperfect contact

$$\begin{cases} -\nabla \cdot \beta(x,y)\nabla u(x,y) + c(x,y)u(x,y) = f(x,y), & x \in \Omega\backslash\Gamma, \\ u(x,y) = g(x,y), & x \in \partial\Omega \end{cases} \tag{1.1}$$

together with the following implicit jump conditions across the interface Γ:

* Received April 29, 2022 / Revised version received October 8, 2022 / Accepted February 12, 2023 / Published online November 1, 2023 /
[1)] Corresponding author

$$\begin{cases} [u] = u^+ - u^- = \lambda \beta^+ \nabla u^+ \cdot \vec{n}, \\ \left[\beta \dfrac{\partial u}{\partial \vec{n}}\right] = \beta^+ \nabla u^+ \cdot \vec{n} - \beta^- \nabla u^- \cdot \vec{n} = 0, \end{cases} \tag{1.2}$$

where $u^{\pm}(x,y) = u(x,y)|_{\Omega^{\pm}}$ and $\vec{n}$ is a unit normal to the interface pointing from Ω^- to Ω^+. Without loss of generality, we assume that $\Omega \subset \mathbb{R}^2$ is a rectangular domain, and the interface Γ is a smooth straight or curve line which separates Ω into two sub-domains Ω^- and Ω^+.

The interface problem (1.1)-(1.2) arises in many important scientific and engineering applications. Examples include incompressible two-phase flow with surface tension featuring jumps in pressure and pressure gradient across the interface [29, 31], temperature discontinuity between gas and cooling solid surface [13], heat conduction between materials of different heat capacity and conductivity and interface diffusion process [24, 32]. It is also applied to model the conjugate heat transfer problem in thermodynamic processes between materials that are thermally coupled through non-adiabatic contacts [9], heat transfer in composite media, heat transfer in building [36], transient behavior for the thermoelastic contact of two rods of dissimilar materials [1]. Moreover, the dielectric heat conduction problem of solid spherical particles dispersed in the continuous phase [25], the calculation of temperature distribution in multi-layer thin film structures [30], e.g. X-ray lithography, laser annealing, laser processing, etc, can also be described by the elliptic interface problem.

The solution of the elliptic interface problems is often discontinuous due to discontinuous coefficients or singular sources across the interface. Various numerical methods are provided for solving these kind of problems. According to the geometric relationship between the computational grid and the material interface, the numerical methods can be generally divided into two categories:

(1) The interface fitted mesh methods [2, 5, 11, 20, 39]. This kind of method features by the computational mesh fits the interface, it means that an element of the underlying mesh is required to intersect with the interface only through its boundaries. This approach is beneficial for the numerical scheme to reach optimal convergence. However, when the geometry is complex, this usually leads to a nontrivial interface meshing problem. Another disadvantage of the fitted mesh is encountered when solving moving interface problems. Since the interface is moving, a new fitted mesh has to be generated at each time step and an interpolation is required to transfer the numerical solutions solved on different meshes.

(2) The interface unfitted mesh method. In this second approach, the interface is allowed to cut computational cells. One difficulty is that special treatment needs to be introduced on these elements in which the interface pass through. And the conditioning of the resulting linear system has a strong dependence on how the interface cuts the mesh cells [4]. There are many interface unfitted mesh methods, such as, the immersed interface method [8, 19, 21, 26, 33], the immersed finite volume method [3,6,23,35,40], and the immersed finite element method [7, 12, 15, 22, 37].

To summarize, elliptic interface problem has been well-studied and can be well solved using finite difference, finite element and finite volume type methods. However, there are significant differences at the connection conditions imposed along the interface. Usually the continuity of the temperature in addition to the conservation of the conductive heat flux are imposed on the interfaces and are referred to as the continuity interface conditions [12, 22] (known as perfect

contact or the homogeneous jump interface conditions, $[u] = 0$, $[\beta \partial u/\partial \vec{n}] = 0$). Besides, the imperfect contact condition with nonhomogeneous jump conditions are frequently imposed along the interface. On this type of interface, the jumps of the temperature as well as the conductive heat flux along the interface are known explicitly [15, 21, 37], (say $[u] = g_1$, $[\beta \partial u/\partial \vec{n}] = g_2$, with known g_1 and g_2). There is another imperfect interface condition [5, 17, 36], which has a continuous heat flux across the interface, while allowing a jump in the temperature and the temperature jump is assumed to be proportional to the average heat flux across the interface, as (1.2). When the elliptic interface problem has a implicit jump condition as in (1.2), there are comparatively few numerical methods for solving such problems.

When the jumps are implicit along the interface problems, numerically solving the governing equations becomes more challenging. It is difficult to use continuous Galerkin method directly on the global domain because of the special interface structure and variational formulation. Some special techniques should be introduced when the nonstandard FEM is used. Javili [14] developed a thermodynamically consistent theory for general imperfect interfaces and to establish a unified computational framework to model all classes of such interfaces using the finite element method. Monsurro [10,27] studied the asymptotic behavior of a problem modelling the stationary diffusion in a two-component heat conductor, with a contact resistance. The flow of heat through the interface separating the two media is supposed to be proportional to the jump of the temperature field. Costa *et al.* [9] proposed a high-order accurate finite volume scheme in general polygonal meshes to solve conjugate heat transfer problems with arbitrary curved interfaces and imperfect thermal contacts. A generic polynomial reconstruction method is used to provide local approximations of the temperature complemented with the reconstruction for off-site data method to properly fulfill the prescribed interface conditions. Jo and Kwak [17] introduced an immersed element method for elliptic interface problems, where the jumps are related to the normal fluxes. The discontinuity of solution is handled by incorporating the implicit jump conditions into a bilinear form through enriching usual P_1 finite element space by extra degrees of freedom on each side of the interface. Kwak and Lee [18] introduced a new variational form and a new finite element method for solving second-order elliptic interface problems where the jump of primary variable is related to the normal flux. The jump conditions along the interface is satisfied by modifying the P_1-Crouzeix-Raviart element. The scheme has consistency and stability terms to compensate the inconsistency along the boundary of the interface elements. Wang [34] proposed a non-traditional finite element method with non-body-fitting grids to solve the elliptic equations with imperfect contact in two dimensions, in which the coefficient $\beta(x)$ is a 2×2 matrix. The method was proved to be second-order accuracy in L_∞ norm, and the condition number of the coefficient matrix grows with order $\mathcal{O}(h^{-2})$. Jia *et al.* [16] proposed a domain decomposition method for the imperfect interface problem and proved that the iterative method is convergent and the iterative procedure is extremum-preserving. Cao *et al.* [5] presented a monotone finite volume scheme for the diffusion equation with imperfect interface which can obtain second-order accuracy solution on the body fitted quadrilateral and triangular meshes.

In this paper, we consider the stationary heat equation in the two component composite modelized by $\Omega, \Omega = \Omega_1 \cup \Omega_2$, and separated by a contact surface Γ, on which the jump of primary variable is proportional to the normal flux across Γ. A finite difference method is constructed for the two dimensional elliptic equations with the imperfect contact. The stability and convergence analysis are provided for the presented scheme. In the case that the interface is straight and the diffusion coefficient is piecewise constant, the presented scheme is proved

to be monotone. The numerical results from the proposed scheme based on the unfitted-mesh method are compared with the results in [5], in which the solution is obtained by finite volume method on the body fitted quadrilateral and triangular meshes. Numerical results show that the presented scheme has roughly second-order accuracy for elliptic interface problems with imperfect contact.

The rest of this paper is organized as follows. In Section 2, we construct the scheme for elliptic equations with straight line and curve type interfaces. Section 3 is devoted to analyze the monotonicity, stability and convergent rate of the scheme. Numerical examples are carried out in Section 4 to demonstrate the accuracy and stability of the presented scheme. A conclusion remark is given in Section 5.

2. Construction of Difference Scheme

2.1. The straight line interface

For simplicity, we start with the case that the interface is a straight line. We assume that $\beta(x,y)$, $c(x,y)$ and $f(x,y)$ are piecewise smooth functions which may have a jump at the interface $x=\alpha$, and $\beta(x,y)$ is bounded

$$0<\beta_{\min}\le\beta(x,y)\le\beta_{\max}, \tag{2.1}$$

where $\beta_{\min}$ and $\beta_{\max}$ are two constants.

Note $\beta(x,y)$ will be assumed to be piecewise constants, and $c(x,y)$ and $f(x,y)$ are continuous in the derivation of the scheme for simplicity.

Assume $x_k<\alpha<x_{k+1}$. Introduce a uniform grid $x_i=ih, y_j=jh$, $i,j=0,1,\ldots,n$ with $h=1/n$. The finite difference scheme can be written as

$$\begin{aligned} L_h u^h_{i,j} &= \gamma_{i,j,1}u^h_{i-1,j}+\gamma_{i,j,2}u^h_{i,j-1}+\gamma_{i,j,3}u^h_{i,j}\\ &\quad+\gamma_{i,j,4}u^h_{i,j+1}+\gamma_{i,j,5}u^h_{i+1,j}+c_{i,j}u^h_{i,j}=f_{i,j}, \end{aligned} \tag{2.2}$$

where $u^h_{i,j}=u^h(x_i,y_j)$ and $i,j=1,2,\ldots,n-1$, $i\neq k,k+1$.

That is, at a regular point, $i\neq k,k+1$, L_h is the usual central (five-point) difference approximation

$$\begin{aligned} &\gamma_{i,j,1}=-\frac{\beta(x_{i-\frac12},y_j)}{h^2},\quad \gamma_{i,j,2}=-\frac{\beta(x_{i+\frac12},y_j)}{h^2},\\ &\gamma_{i,j,3}=-(\gamma_{i,j,1}+\gamma_{i,j,2}+\gamma_{i,j,4}+\gamma_{i,j,5}),\\ &\gamma_{i,j,4}=-\frac{\beta(x_i,y_{j-\frac12})}{h^2},\quad \gamma_{i,j,5}=-\frac{\beta(x_i,y_{j+\frac12})}{h^2},\quad f_{i,j}=f(x_i,y_j), \end{aligned}$$

where

$$x_{i-\frac12}=\frac{x_i+x_{i-1}}{2},\quad y_{i-\frac12}=\frac{y_i+y_{i-1}}{2},\quad i,j=1,2,\ldots,n.$$

The local truncation error is $\mathcal{O}(h^2)$

$$\begin{aligned} T_{i,j} &= \gamma_{i,j,1}u^h_{i-1,j}+\gamma_{i,j,2}u^h_{i,j-1}+\gamma_{i,j,3}u^h_{i,j}+\gamma_{i,j,4}u^h_{i,j+1}\\ &\quad+\gamma_{i,j,5}u^h_{i+1,j}+c_{i,j}u^h_{i,j}-f_{i,j}=\mathcal{O}(h^2),\quad i\neq k,k+1. \end{aligned}$$

At the irregular grid point $(x_k, y_j), j = 1, 2, \ldots, n$, we introduce the following seven-point stencil:

$$\gamma_1 u^h_{i-1,j} + \gamma_2 u^h_{i,j-1} + \gamma_3 u^h_{i,j} + \gamma_4 u^h_{i,j+1} + \gamma_5 u^h_{i+1,j} + \gamma_6 u^h_{k+1j} + \gamma_7 u^h_{k+1,j+1} + c_{k,j} u^h_{k,j} = f_{k,j} + R_{k,j},$$

where the coefficients γ_s should depend on k, j, but for simplicity of notation we drop these indices, and they will be determined as follows.

For a function $u(x, y)$, denote

$$u_{i,j} = u(x_i, y_j), \quad u^-_j = u(\alpha^-, y_j), \quad u^+_j = u(\alpha^+, y_j).$$

Besides, the stencil points $(k-1, j)$, $(k, j-1)$, (k, j), $(k, j+1)$, $(k+1, j-1)$, $(k+1, j)$, $(k+1, j+1)$ are respectively denoted by $1, 2, 3, 4, 5, 6, 7$, respectively, see Fig. 2.1(a). Thus, the functions $u_{k-1,j}, u_{k,j-1}, u_{k,j}, u_{k+1,j-1}, u_{k,j+1}, u_{k+1,j}, u_{k+1,j+1}$ can be written as $u_1, u_2, u_3, u_4, u_5, u_6, u_7$, respectively.

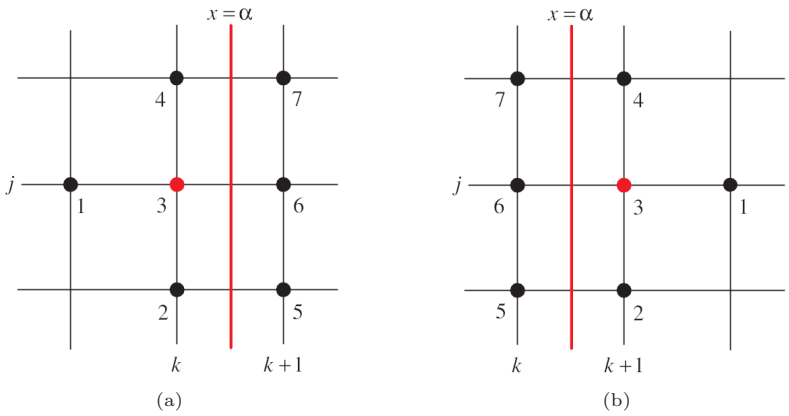

Fig. 2.1. The stencils for the irregular points (a) (k, j) and (b) $(k + 1, j)$ with straight line interface.

Expand $u_{k-1,j}, u_{k,j-1}, u_{k,j}, u_{k+1,j-1}, u_{k,j+1}, u_{k+1,j}$ and $u_{k+1,j+1}$ in Taylor series about the point (α, y_j)

$$u_m = u^- + h_{x,m} u^-_x + h_{y,m} u^-_y + \frac{h^2_{x,m}}{2} u^-_{xx} + \frac{h_{x,m} h_{y,m}}{2} u^-_{xy} + \frac{h^2_{y,m}}{2} u^-_{yy} + \mathcal{O}(h^3), \quad m \in \Omega^-, \tag{2.3}$$

$$u_m = u^+ + h_{x,m} u^+_x + h_{y,m} u^+_y + \frac{h^2_{x,m}}{2} u^+_{xx} + \frac{h_{x,m} h_{y,m}}{2} u^+_{xy} + \frac{h^2_{y,m}}{2} u^+_{yy} + \mathcal{O}(h^3), \quad m \in \Omega^+, \tag{2.4}$$

where $h_{x,m} = x_m - \alpha$, $h_{y,m} = y_m - y_i$.

From the interface connecting condition (1.2), it follows:

$$u^+ = u^- + \lambda \beta^- u^-_x, \quad u^+_x = \frac{\beta^- u^-_x}{\beta^+},$$

$$
\begin{aligned}
u_y^+ &= \lambda\beta_y^- u_x^- + u_y^- + \lambda\beta^- u_{xy}^-,\\
u_{xy}^+ &= \frac{\beta_y^-\beta^+ - \beta^-\beta_y^+}{{\beta^+}^2}u_x^- + \frac{\beta^-}{\beta^+}u_{xy}^-,\\
u_{yy}^+ &= \lambda\beta_{yy}^- u_x^- + 2\lambda\beta_y^- u_{xy}^- + u_{yy}^- + \lambda\beta^- u_{xyy}^-.
\end{aligned}
$$

Moreover, the governing equation (1.1) yields

$$
\begin{aligned}
&-\beta^+u_{xx}^+ - \beta^+u_{yy}^+ - \beta_x^+u_x^+ - \beta_y^+u_y^+ + c^+u^+ - f^+\\
&= -\beta^-u_{xx}^- - \beta^-u_{yy}^- - \beta_x^-u_x^- - \beta_y^-u_y^- + c^-u^- - f^-.
\end{aligned}
$$

Hence,

$$
\begin{aligned}
u_{xx}^+ &= \frac{[c]}{\beta^+}u^- + \frac{1}{\beta^+}\left\{\frac{\beta_x^-\beta^+ - \beta_x^+\beta^-}{\beta^+} - \lambda\beta_y^+\beta_y^- - \lambda\beta^+\beta_{yy}^- + \lambda c^+\beta^-\right\}u_x^- - \frac{[\beta_y]}{\beta^+}u_y^-\\
&\quad + \frac{\beta^-}{\beta^+}u_{xx}^- - \frac{[\beta]}{\beta^+}u_{yy}^- - \frac{\lambda\beta^-\beta_y^+ + 2\lambda\beta^+\beta_y^-}{\beta^+}u_{xy}^- - \lambda\beta^-u_{xyy}^- - \frac{[f]}{\beta^+},\\
u_{xx}^- &= -\frac{[c]}{\beta^-}u^+ + \frac{1}{\beta^-}\left\{\frac{\beta_x^+\beta^- - \beta_x^-\beta^+}{\beta^-} + \lambda\beta_y^-\beta_y^+ + \lambda\beta^-\beta_{yy}^+ - \lambda c^-\beta^+\right\}u_x^+ + \frac{[\beta_y]}{\beta^-}u_y^+\\
&\quad + \frac{\beta^+}{\beta^-}u_{xx}^+ + \frac{[\beta]}{\beta^-}u_{yy}^+ + \frac{\lambda\beta^+\beta_y^- + 2\lambda\beta^-\beta_y^+}{\beta^-}u_{xy}^+ + \lambda\beta^+u_{xyy}^+ + \frac{[f]}{\beta^-}.
\end{aligned}
$$

By representing u^+ with u^-, the Taylor expression (2.3) and (2.4) can be rewritten as

$$
\begin{aligned}
u_m &= \omega_{m,1}u^- + \omega_{m,2}u_x^- + \omega_{m,3}u_y^- + \omega_{m,4}u_{xx}^- + \omega_{m,5}u_{xy}^-\\
&\quad + \omega_{m,6}u_{yy}^- + \omega_{m,7}u_{xyy}^- + G_m + \mathcal{O}(h^3), \quad m = 1,2,\ldots,7,
\end{aligned}
\tag{2.5}
$$

where

$$
\begin{aligned}
&\omega_{1,1} = 1, \quad \omega_{1,2} = h_{x,1}, \quad \omega_{1,3} = 0, \qquad \omega_{1,4} = \frac{h_{x,1}^2}{2},\\
&\omega_{1,5} = \omega_{1,6} = \omega_{1,7} = 0,\\
&\omega_{2,1} = 1, \quad \omega_{2,2} = h_{x,2}, \quad \omega_{2,3} = -h, \quad \omega_{2,4} = \frac{h_{x,2}^2}{2},\\
&\omega_{2,5} = \frac{-hh_{x,2}}{2}, \quad \omega_{2,6} = \frac{h^2}{2}, \quad \omega_{2,7} = 0,\\
&\omega_{3,1} = 1, \quad \omega_{3,2} = h_{x,3}, \quad \omega_{3,3} = 0, \qquad \omega_{3,4} = \frac{h_{x,3}^2}{2},\\
&\omega_{3,5} = \omega_{3,6} = \omega_{3,7} = 0,\\
&\omega_{4,1} = 1, \quad \omega_{4,2} = h_{x,4}, \quad \omega_{4,3} = h, \qquad \omega_{4,4} = \frac{h_{x,4}^2}{2},\\
&\omega_{4,5} = \frac{hh_{x,4}}{2}, \qquad \omega_{4,6} = \frac{h^2}{2}, \quad \omega_{4,7} = 0,\\
&G_1 = G_2 = G_3 = G_4 = 0, \quad \omega_{5,1} = 1 + \frac{[c]}{\beta^+}\frac{h_{x,5}^2}{2},\\
&\omega_{5,2} = \lambda\beta^- + \frac{\beta^-}{\beta^+}h_{x,5} - h\lambda\beta_y^- + \frac{h_{x,5}^2}{2\beta^+}\left\{\frac{\beta_x^-\beta^+ - \beta_x^+\beta^-}{\beta^+} - \lambda\beta_y^+\beta_y^- - \lambda\beta^+\beta_{yy}^- + \lambda c^+\beta^-\right\}
\end{aligned}
$$

$$
\begin{aligned}
&\quad - \frac{h_{x,5}h}{2}\frac{\beta_y^-\beta^+ - \beta^-\beta_y^+}{{\beta^+}^2} + \lambda\beta_{yy}^-\frac{h^2}{2},\\
\omega_{5,3} &= -h - \frac{h_{x,5}^2}{2}\frac{[\beta_y]}{\beta^+}, \quad \omega_{5,4} = \frac{h_{x,5}^2}{2}\frac{\beta^-}{\beta^+},\\
\omega_{5,5} &= -\lambda h\beta^- - \frac{h_{x,5}^2}{2}\frac{\lambda\beta^-\beta_y^+ + 2\lambda\beta^+\beta_y^-}{\beta^+} - \frac{\beta^-}{\beta^+}\frac{hh_{x,5}}{2} + \lambda h^2\beta_y^-,\\
\omega_{5,6} &= \frac{h^2}{2} - \frac{h_{x,5}^2}{2}\frac{[\beta]}{\beta^+}, \quad \omega_{5,7} = \lambda\beta^-\frac{h^2}{2} - \lambda\beta^-\frac{h_{x,5}^2}{2},\\
G_5 &= -\frac{[f]}{\beta^+}\frac{h_{x,5}^2}{2}, \quad \omega_{6,1} = 1 + \frac{h_{x,6}^2}{2}\frac{[c]}{\beta^+},\\
\omega_{6,2} &= \lambda\beta^- + \frac{\beta^-}{\beta^+}h_{x,6} + \frac{h_{x,6}^2}{2\beta^+}\left\{\frac{\beta_x^-\beta^+ - \beta_x^+\beta^-}{\beta^+} - \lambda\beta_y^+\beta_y^- - \lambda\beta^+\beta_{yy}^- + \lambda c^+\beta^-\right\},\\
\omega_{6,3} &= -\frac{h_{x,6}^2}{2}\frac{[\beta_y]}{\beta^+}, \qquad \omega_{6,4} = \frac{h_{x,6}^2}{2}\frac{\beta^-}{\beta^+}, \quad \omega_{6,5} = -\frac{h_{x,6}^2}{2}\frac{\lambda\beta^-\beta_y^+ + 2\lambda\beta^+\beta_y^-}{\beta^+},\\
\omega_{6,6} &= -\frac{h_{x,6}^2}{2}\frac{[\beta]}{\beta^+}, \qquad \omega_{6,7} = -\frac{h_{x,6}^2}{2}\lambda\beta^-,\\
G_6 &= -\frac{[f]}{\beta^+}\frac{h_{x,6}^2}{2}, \quad \omega_{7,1} = 1 + \frac{h_{x,7}^2}{2}\frac{[c]}{\beta^+},\\
\omega_{7,2} &= \lambda\beta^- + \frac{\beta^-}{\beta^+}h_{x,7} + \lambda h\beta_y^- + \frac{h_{x,7}^2}{2\beta^+}\left\{\frac{\beta_x^-\beta^+ - \beta_x^+\beta^-}{\beta^+} - \lambda\beta_y^+\beta_y^- - \lambda\beta^+\beta_{yy}^- + \lambda c^+\beta^-\right\}\\
&\quad + \frac{hh_{x,7}}{2}\frac{\beta_y^-\beta^+ - \beta^-\beta_y^+}{{\beta^+}^2} + \lambda\beta_{yy}^-\frac{h^2}{2},\\
\omega_{7,3} &= h - \frac{h_{x,7}^2}{2}\frac{[\beta_y]}{\beta^+}, \quad \omega_{7,4} = \frac{h_{x,7}^2}{2}\frac{\beta^-}{\beta^+},\\
\omega_{7,5} &= \lambda h\beta^- - \frac{h_{x,7}^2}{2}\frac{\lambda\beta^-\beta_y^+ + 2\lambda\beta^+\beta_y^-}{\beta^+} + \frac{\beta^-}{\beta^+}\frac{hh_{x,7}}{2} + \lambda h^2\beta_y^-,\\
\omega_{7,6} &= \frac{h^2}{2} - \frac{h_{x,7}^2}{2}\frac{[\beta]}{\beta^+}, \quad \omega_{7,7} = \lambda\beta^-\frac{h^2}{2} - \lambda\beta^-\frac{h_{x,7}^2}{2}, \quad G_7 = -\frac{[f]}{\beta^+}\frac{h_{x,7}^2}{2}.
\end{aligned}
$$

Substitute these expressions into the local truncation error $T_{k,j}$, and then collect terms according to the of combination coefficients of $u^-, u_x^-, u_y^-, u_{xx}^-, u_{yy}^-, u_{xy}^-$ and u_{xyy}^-. There is

$$
\begin{aligned}
T_{k,j} &= \gamma_1 u_1 + \gamma_2 u_2 + \gamma_3 u_3 + \gamma_4 u_4 + \gamma_5 u_5 + \gamma_6 u_6 + \gamma_7 u_7\\
&\quad - (-\beta_x^- u_x^- - \beta^- u_{xx}^- - \beta_y^- u_y^- - \beta^- u_{yy}^-) - R_{k,j}\\
&= (\gamma_1\omega_{1,1} + \gamma_2\omega_{2,1} + \gamma_3\omega_{3,1} + \gamma_4\omega_{4,1} + \gamma_5\omega_{5,1} + \gamma_6\omega_{6,1} + \gamma_7\omega_{7,1})u^-\\
&\quad + (\gamma_1\omega_{1,2} + \gamma_2\omega_{2,2} + \gamma_3\omega_{3,2} + \gamma_4\omega_{4,2} + \gamma_5\omega_{5,2} + \gamma_6\omega_{6,2} + \gamma_7\omega_{7,2} + \beta_x^-)u_x^-\\
&\quad + (\gamma_1\omega_{1,3} + \gamma_2\omega_{2,3} + \gamma_3\omega_{3,3} + \gamma_4\omega_{4,3} + \gamma_5\omega_{5,3} + \gamma_6\omega_{6,3} + \gamma_7\omega_{7,3} + \beta_y^-)u_y^-\\
&\quad + (\gamma_1\omega_{1,4} + \gamma_2\omega_{2,4} + \gamma_3\omega_{3,4} + \gamma_4\omega_{4,4} + \gamma_5\omega_{5,4} + \gamma_6\omega_{6,4} + \gamma_7\omega_{7,4} + \beta^-)u_{xx}^-\\
&\quad + (\gamma_2\omega_{2,5} + \gamma_4\omega_{4,5} + \gamma_5\omega_{5,5} + \gamma_6\omega_{6,5} + \gamma_7\omega_{7,5})u_{xy}^-\\
&\quad + (\gamma_2\omega_{2,6} + \gamma_4\omega_{4,6} + \gamma_5\omega_{5,6} + \gamma_6\omega_{6,6} + \gamma_7\omega_{7,6} + \beta^-)u_{yy}^-\\
&\quad + (\gamma_5\omega_{5,7} + \gamma_6\omega_{6,7} + \gamma_7\omega_{7,7})u_{xyy}^-\\
&\quad + (\gamma_5 G_5 + \gamma_6 G_6 + \gamma_7 G_7 - R_{k,j}) + \mathcal{O}(h).
\end{aligned}
$$

To require $T_{k,j}$ being $\mathcal{O}(h)$, we get the following linear system with unknown γ_s $(1 \le s \le 7)$:

$$\begin{pmatrix} \omega_{1,1} & \omega_{2,1} & \omega_{3,1} & \omega_{4,1} & \omega_{5,1} & \omega_{6,1} & \omega_{7,1} \\ \omega_{1,2} & \omega_{2,2} & \omega_{3,2} & \omega_{4,2} & \omega_{5,2} & \omega_{6,2} & \omega_{7,2} \\ 0 & -h & 0 & h & \omega_{5,3} & \omega_{6,3} & \omega_{7,3} \\ \omega_{1,4} & \omega_{2,4} & \omega_{3,4} & \omega_{4,4} & \omega_{5,4} & \omega_{6,4} & \omega_{7,4} \\ 0 & -\dfrac{hh_{x,1}}{2} & 0 & \dfrac{hh_{x,1}}{2} & \omega_{5,5} & \omega_{6,5} & \omega_{7,5} \\ 0 & \dfrac{h^2}{2} & 0 & \dfrac{h^2}{2} & \omega_{5,6} & \omega_{6,6} & \omega_{7,6} \\ 0 & 0 & 0 & 0 & \omega_{5,7} & \omega_{6,7} & \omega_{7,7} \end{pmatrix} \begin{pmatrix} \gamma_1 \\ \gamma_2 \\ \gamma_3 \\ \gamma_4 \\ \gamma_5 \\ \gamma_6 \\ \gamma_7 \end{pmatrix} = \begin{pmatrix} 0 \\ -\beta_x^- \\ -\beta_y^- \\ -\beta^- \\ 0 \\ -\beta^+ \\ 0 \end{pmatrix}. \tag{2.6}$$

If $\beta_x^- = \beta_x^+ = 0$, $\beta_y^- = \beta_y^+ = 0$ and $c(x,y)$ is continuous, the linear system can be written as

$$\begin{cases} \gamma_1 + \gamma_2 + \gamma_3 + \gamma_4 + \gamma_5 + \gamma_6 + \gamma_7 = 0, \\ h_{x,1}\gamma_1 + h_{x,2}(\gamma_2 + \gamma_3 + \gamma_4) + \left(\lambda\beta^- + \dfrac{\beta^-}{\beta^+}h_{x,5} + \dfrac{\lambda c^+\beta^-}{\beta^+}\dfrac{h_{x,5}^2}{2}\right)(\gamma_5 + \gamma_6 + \gamma_7) = 0, \\ -\gamma_2 + \gamma_4 - \gamma_5 + \gamma_7 = 0, \\ h_{x,1}^2\gamma_1 + h_{x,2}^2(\gamma_2 + \gamma_3 + \gamma_4) + \dfrac{\beta^-}{\beta^+}h_{x,5}^2(\gamma_5 + \gamma_6 + \gamma_7) = -2\beta^-, \\ h_{x,2}(-\gamma_2 + \gamma_4) + \left(\lambda\beta^- + \dfrac{\beta^-}{\beta^+}h_{x,5}\right)(-\gamma_5 + \gamma_7) = 0, \\ h^2(\gamma_2 + \gamma_4) + \left(h^2 - \dfrac{[\beta]}{\beta^+}h_{x,5}^2\right)(\gamma_5 + \gamma_7) - \dfrac{[\beta]}{\beta^+}h_{x,5}^2\gamma_6 = -2\beta^+, \\ (h^2 - h_{x,5}^2)(\gamma_5 + \gamma_7) - h_{x,5}^2\gamma_6 = 0, \end{cases}$$

and

$$R_{k,j} = (\gamma_5 + \gamma_6 + \gamma_7)\left(-\frac{(x_{k+1} - \alpha)^2}{2\beta^+}[f]\right).$$

At the irregular points (x_{k+1}, y_j), $j = 1, 2, \ldots, n$, similar finite difference scheme can be introduced, i.e.

$$\begin{aligned} &\bar\gamma_1 u_{k+2_j}^h + \bar\gamma_2 u_{k+1,j-1}^h + \bar\gamma_3 u_{k+1,j}^h + \bar\gamma_4 u_{k+1,j+1}^h + \bar\gamma_5 u_{k,j-1}^h + \bar\gamma_6 u_{k,j}^h \\ &\quad + \bar\gamma_7 u_h(x_k, y_{j+1}) + c_{k+1,j}u_{k+1,j}^h = f_{k+1,j} + R_{k+1,j}. \end{aligned}$$

Denote the 7 points $(k+2,j), (k+1,j-1), (k+1,j), (k+1,j+1), (k,j-1), (k,j), (k,j+1)$ as $1, 2, 3, 4, 5, 6, 7$, respectively, see Fig. 2.1(b). Expand $u_{k+2,j}$, $u_{k+1,j-1}$, $u_{k+1,j}$, $u_{k+1,j+1}$, $u_{k,j-1}$, $u_{k,j}$ and $u_{k,j+1}$ in Taylor series at point (α, j). These Taylor expression can be rewritten as

$$\begin{aligned} u_m = {} & \bar\omega_{m,1}u^+ + \bar\omega_{m,2}u_x^+ + \bar\omega_{m,3}u_y^+ + \bar\omega_{m,4}u_{xx}^+ + \bar\omega_{m,5}u_{xy}^+ \\ & + \bar\omega_{m,6}u_{yy}^+ + \bar\omega_{m,7}u_{xyy}^+ + \bar G_m + \mathcal{O}(h^3), \quad m = 1, 2, \ldots, 7, \end{aligned} \tag{2.7}$$

where

$$\bar\omega_{1,1} = 1, \quad \bar\omega_{1,2} = h_{x,1}, \quad \bar\omega_{1,3} = 0, \qquad \bar\omega_{1,4} = \frac{h_{x,1}^2}{2},$$
$$\bar\omega_{1,5} = \bar\omega_{1,6} = \bar\omega_{1,7} = 0,$$

$$\bar{\omega}_{2,1}=1,\quad \bar{\omega}_{2,2}=h_{x,2},\quad \bar{\omega}_{2,3}=-h,\quad \bar{\omega}_{2,4}=\frac{h_{x,2}^2}{2},$$

$$\bar{\omega}_{2,5}=-\frac{hh_{x,2}}{2},\quad \bar{\omega}_{2,6}=\frac{h^2}{2},\quad \bar{\omega}_{2,7}=0,$$

$$\bar{\omega}_{3,1}=1,\quad \bar{\omega}_{3,2}=h_{x,3},\quad \bar{\omega}_{3,3}=0,\qquad \bar{\omega}_{3,4}=\frac{h_{x,3}^2}{2},$$

$$\bar{\omega}_{3,5}=\bar{\omega}_{3,6}=\bar{\omega}_{3,7}=0,$$

$$\bar{\omega}_{4,1}=1,\quad \bar{\omega}_{4,2}=h_{x,4},\quad \bar{\omega}_{4,3}=h,\qquad \bar{\omega}_{4,4}=\frac{h_{x,4}^2}{2},$$

$$\bar{\omega}_{4,5}=\frac{hh_{x,4}}{2},\qquad \bar{\omega}_{4,6}=\frac{h^2}{2},\quad \bar{\omega}_{4,7}=0,$$

$$\bar{G}_1=\bar{G}_2=\bar{G}_3=\bar{G}_4=0,\quad \bar{\omega}_{5,1}=1-\frac{[c]}{\beta^-}h_{x,5}^2,$$

$$\bar{\omega}_{5,2}=-\lambda\beta^+ +\frac{\beta^-}{\beta^+}h_{x,5}+\lambda\beta_y^+h+\frac{h_{x,5}^2}{2\beta^-}\left\{\frac{\beta_x^+\beta^- -\beta_x^-\beta^+}{\beta^-}+\lambda\beta_y^-\beta_y^+ +\lambda\beta^-\beta_{yy}^+ -\lambda c^-\beta^+\right\}$$
$$-\frac{hh_{x,5}}{2}\frac{\beta_y^+\beta^- -\beta_y^-\beta^+}{{\beta^-}^2}-\lambda\beta_{yy}^+\frac{h^2}{2},$$

$$\bar{\omega}_{5,3}=-h+\frac{h_{x,5}^2}{2}\frac{[\beta_y]}{\beta^-},\quad \bar{\omega}_{5,4}=-\frac{h_{x,5}^2}{2}\frac{\beta^+}{\beta^-},$$

$$\bar{\omega}_{5,5}=\lambda h\beta^+ +\frac{h_{x,5}^2}{2}\frac{\lambda\beta_y^-\beta^+ +2\lambda\beta^-\beta_y^+}{\beta^-}-\frac{\beta^+}{\beta^-}\frac{hh_{x,5}}{2}-\lambda h^2\beta_y^+,$$

$$\bar{\omega}_{5,6}=\frac{h^2}{2}+\frac{[\beta]}{\beta^-}\frac{h_{x,5}^2}{2},\qquad \bar{\omega}_{5,7}=\lambda\beta^+\frac{h_{x,5}^2}{2}-\lambda\beta^+\frac{h^2}{2},$$

$$\bar{G}_5=\frac{[f]}{\beta^-}\frac{h_{x,5}^2}{2},\quad \bar{\omega}_{6,1}=1-\frac{[c]}{\beta^-}\frac{h_{x,6}^2}{2},$$

$$\bar{\omega}_{6,2}=-\lambda\beta^+ +\frac{\beta^+}{\beta^-}h_{x,6}+\frac{h_{x,6}^2}{2\beta^-}\left\{\frac{\beta_x^+\beta^- -\beta_x^-\beta^+}{\beta^-}+\lambda\beta_y^-\beta_y^+ +\lambda\beta^-\beta_{yy}^+ -\lambda c^-\beta^+\right\},$$

$$\bar{\omega}_{6,3}=\frac{h_{x,6}^2}{2}\frac{[\beta_y]}{\beta^-},\qquad \bar{\omega}_{6,4}=-\frac{h_{x,6}^2}{2}\frac{\beta^+}{\beta^-},\quad \bar{\omega}_{6,5}=\frac{h_{x,6}^2}{2}\frac{\lambda\beta_y^-\beta^+ +2\lambda\beta^-\beta_y^+}{\beta^-},$$

$$\bar{\omega}_{6,6}=\frac{h_{x,6}^2}{2}\frac{[\beta]}{\beta^-},\qquad \bar{\omega}_{6,7}=\frac{h_{x,6}^2}{2}\lambda\beta^+,\quad \bar{G}_6=\frac{h_{x,6}^2}{2}\frac{[f]}{\beta^-},\quad \bar{\omega}_{7,1}=1-\frac{[c]}{\beta^-}\frac{h_{x,7}^2}{2},$$

$$\bar{\omega}_{7,2}=-\lambda\beta^+ +\frac{\beta^+}{\beta^-}h_{x,7}-\lambda h\beta_y^+ +\frac{h_{x,7}^2}{2\beta^-}\left\{\frac{\beta_x^+\beta^- -\beta_x^-\beta^+}{\beta^-}+\lambda\beta_y^-\beta_y^+ +\lambda\beta^-\beta_{yy}^+ -\lambda c^-\beta^+\right\}$$
$$+\frac{hh_{x,7}}{2}\frac{\beta_y^+\beta^- -\beta^+\beta_y^-}{{\beta^-}^2}-\lambda\beta_{yy}^+\frac{h^2}{2},$$

$$\bar{\omega}_{7,3}=h+\frac{h_{x,7}^2}{2}\frac{[\beta_y]}{\beta^-},\qquad \bar{\omega}_{7,4}=-\frac{\beta^+}{\beta^-}\frac{h_{x,7}^2}{2},$$

$$\bar{\omega}_{7,5}=-\lambda h\beta^+ +\frac{h_{x,7}^2}{2}\frac{\lambda\beta_y^-\beta^+ +2\lambda\beta^-\beta_y^+}{\beta^-}+\frac{hh_{x,7}}{2}\frac{\beta^+}{\beta^-}-\lambda h^2\beta_y^+,$$

$$\bar{\omega}_{7,6}=\frac{h^2}{2}+\frac{h_{x,7}^2}{2}\frac{[\beta]}{\beta^-},\quad \bar{\omega}_{7,7}=\lambda\beta^+\frac{h_{x,7}^2}{2}-\lambda\beta^+\frac{h^2}{2},\quad \bar{G}_7=\frac{h_{x,7}^2}{2}\frac{[f]}{\beta^-}.$$

Similarly, the coefficients of the scheme at irregular points (x_{k+1}, y_j) are determined by the following system:

$$\begin{pmatrix} \bar{\omega}_{1,1} & \bar{\omega}_{2,1} & \bar{\omega}_{3,1} & \bar{\omega}_{4,1} & \bar{\omega}_{5,1} & \bar{\omega}_{6,1} & \bar{\omega}_{7,1} \\ \bar{\omega}_{1,2} & \bar{\omega}_{5,2} & \bar{\omega}_{5,2} & \bar{\omega}_{5,2} & \bar{\omega}_{5,2} & \bar{\omega}_{6,2} & \bar{\omega}_{7,2} \\ 0 & -h & 0 & h & \bar{\omega}_{5,3} & \bar{\omega}_{6,3} & \bar{\omega}_{7,3} \\ \bar{\omega}_{1,4} & \bar{\omega}_{2,4} & \bar{\omega}_{3,4} & \bar{\omega}_{4,4} & \bar{\omega}_{5,4} & \bar{\omega}_{6,4} & \bar{\omega}_{7,4} \\ 0 & -\dfrac{hh_{x,1}}{2} & 0 & \dfrac{hh_{x,1}}{2} & \bar{\omega}_{5,5} & \bar{\omega}_{6,5} & \bar{\omega}_{7,5} \\ 0 & \dfrac{h^2}{2} & 0 & \dfrac{h^2}{2} & \bar{\omega}_{5,6} & \bar{\omega}_{6,6} & \bar{\omega}_{7,6} \\ 0 & 0 & 0 & 0 & \bar{\omega}_{5,7} & \bar{\omega}_{6,7} & \bar{\omega}_{7,7} \end{pmatrix} \begin{pmatrix} \bar{\gamma}_1 \\ \bar{\gamma}_2 \\ \bar{\gamma}_3 \\ \bar{\gamma}_4 \\ \bar{\gamma}_5 \\ \bar{\gamma}_6 \\ \bar{\gamma}_7 \end{pmatrix} = \begin{pmatrix} 0 \\ -\beta_x^- \\ -\beta_y^- \\ -\beta^- \\ 0 \\ -\beta^+ \\ 0 \end{pmatrix}. \tag{2.8}$$

If $\beta_x^- = \beta_x^+ = 0$, $\beta_y^- = \beta_y^+ = 0$ and $c(x, y)$ is continuous, the linear system can be written as

$$\begin{cases} \bar{\gamma}_1 + \bar{\gamma}_2 + \bar{\gamma}_3 + \bar{\gamma}_4 + \bar{\gamma}_5 + \bar{\gamma}_6 + \bar{\gamma}_7 = 0, \\ h_{x,1}\bar{\gamma}_1 + h_{x,2}(\bar{\gamma}_2 + \bar{\gamma}_3 + \bar{\gamma}_4) + \left(-\lambda\beta^+ + \dfrac{\beta^+}{\beta^-}h_{x,5} - \dfrac{\lambda c^-\beta^+}{\beta^-}\dfrac{h_{x,5}^2}{2} \right)(\bar{\gamma}_5 + \bar{\gamma}_6 + \bar{\gamma}_7) = 0, \\ -\bar{\gamma}_2 + \bar{\gamma}_4 - \bar{\gamma}_5 + \bar{\gamma}_7 = 0, \\ h_{x,1}^2\bar{\gamma}_1 + h_{x,2}^2(\bar{\gamma}_2 + \bar{\gamma}_3 + \bar{\gamma}_4) - \dfrac{\beta^+}{\beta^-}h_{x,5}^2(\bar{\gamma}_5 + \bar{\gamma}_6 + \bar{\gamma}_7) = -2\beta^-, \\ h_{x,2}(-\bar{\gamma}_2 + \bar{\gamma}_4) + \left(-\lambda\beta^+ + \dfrac{\beta^+}{\beta^-}h_{x,5} \right)(-\bar{\gamma}_5 + \bar{\gamma}_7) = 0, \\ h^2(\bar{\gamma}_2 + \bar{\gamma}_4) + \left(\dfrac{[\beta]}{\beta^-}h_{x,5}^2 + h^2 \right)(\bar{\gamma}_5 + \bar{\gamma}_7) + \dfrac{[\beta]}{\beta^-}h_{x,5}^2\gamma_6 = -2\beta^+, \\ \left(h_{x,5}^2 - h^2\right)(\bar{\gamma}_5 + \bar{\gamma}_7) + h_{x,5}^2\bar{\gamma}_6 = 0, \end{cases}$$

and

$$R_{k+1,j} = (\bar{\gamma}_5 + \bar{\gamma}_6 + \bar{\gamma}_7)\left(\frac{(x_k - \alpha)^2}{2\beta^-}[f] \right).$$

2.2. The curved interface

In this section, we consider the interface Γ be piecewise smooth curve. Before proceeding to the construction of the numerical scheme for u_{xx} or u_{yy} at irregular grid points, we first rewrite the interface jump conditions as two separate conditions for $[u_x]_\Gamma$ and $[u_y]_\Gamma$. Denote $\vec{n}$ be the unit normal of the interface from Ω^- to Ω^+, $\vec{n} = (n_1, n_2)$. The tangential direction of the interface can be defined as $\vec{\tau} = (-n_2, n_1)$. Then, the interface connection condition can be given as following:

$$[u] = u^+ - u^- = \lambda\beta^-\frac{\partial u^-}{\partial \vec{n}} = \lambda\beta^-(u_x^- n_1 + u_y^- n_2), \tag{2.9}$$

$$\beta^-\frac{\partial u^-}{\partial \vec{n}} = \beta^+\frac{\partial u^+}{\partial \vec{n}}. \tag{2.10}$$

Differentiating interface jump condition $[u]$ along the tangential direction of the interface, we obtain

$$[u_{\vec{\tau}}] = [u_y]n_1 - [u_x]n_2 = Q, \tag{2.11}$$

where

$$Q = \lambda(\beta_y^- n_1^2 - \beta_x^- n_1 n_2)u_x^- + \lambda(\beta_y^- n_1 n_2 - \beta_x^- n_2^2)u_y^- - \lambda\beta^- n_1 n_2 u_{xx}^- + \lambda\beta^-(n_1^2 - n_2^2)u_{xy}^- + \lambda\beta^- n_1 n_2 u_{yy}^-.$$

Eq. (2.10) can be rewritten as

$$\beta^+ u_x^+ n_1 + \beta^+ u_y^+ n_2 = \beta^- u_x^- n_1 + \beta^- u_y^- n_2. \tag{2.12}$$

Moreover, we rewrite (2.11) as

$$u_y^+ n_1 - u_x^+ n_2 = Q + u_y^- n_1 - u_x^- n_2. \tag{2.13}$$

Multiplying (2.13) by β^+ gives

$$\beta^+ u_y^+ n_1 - \beta^+ u_x^+ n_2 = \beta^+(Q + u_y^- n_1 - u_x^- n_2).$$

Solve the following linear system:

$$\begin{cases} \beta^+ u_x^+ n_1 + \beta^+ u_y^+ n_2 = \beta^- u_x^- n_1 + \beta^- u_y^- n_2, \\ \beta^+ u_y^+ n_1 - \beta^+ u_x^+ n_2 = \beta^+(Q + u_y^- n_1 - u_x^- n_2). \end{cases}$$

The $\beta^+ u_x^+$ and $\beta^+ u_y^+$ are given as

$$\begin{aligned} \beta^+ u_x^+ &= (\beta^- u_x^- n_1 + \beta^- u_y^- n_2)n_1 - [\beta^+(Q + u_y^- n_1 - u_x^- n_2)]n_2 \\ &= \big(\beta^- n_1^2 + \beta^+ n_2^2\big)u_x^- + (\beta^- - \beta^+)n_1 n_2 u_y^- - \beta^+ Q n_2 \\ &= \Big\{\big(\beta^- n_1^2 + \beta^+ n_2^2\big) - \lambda\beta^+\big(\beta_y^- n_1^2 n_2 - \beta_x^- n_1 n_2^2\big)\Big\}u_x^- \\ &\quad + \Big\{(\beta^- - \beta^+)n_1 n_2 - \lambda\beta^+\big(\beta_y^- n_1 n_2^2 - \beta_x^- n_2^3\big)\Big\}u_y^- \\ &\quad + \lambda\beta^-\beta^+ n_1 n_2^2 u_{xx}^- - \lambda\beta^-\beta^+\big(n_1^2 - n_2^2\big)n_2 u_{xy}^- - \lambda\beta^+\beta^- n_1 n_2^2 u_{yy}^-, \end{aligned}$$

and

$$\begin{aligned} \beta^+ u_y^+ &= [\beta^+(Q + u_y^- n_1 - u_x^- n_2)]n_1 + (\beta^- u_x^- n_1 + \beta^- u_y^- n_2)n_2 \\ &= u_x^- n_1 n_2(\beta^- - \beta^+) + u_y^-\big(\beta^+ n_1^2 + \beta^- n_2^2\big) + \beta^+ Q n_1 \\ &= \Big\{(\beta^- - \beta^+)n_1 n_2 + \lambda\beta^+ n_1\big(\beta_y^- n_1^2 - \beta_x^- n_1 n_2\big)\Big\}u_x^- \\ &= \Big\{\big(\beta^+ n_1^2 + \beta^- n_2^2\big) + \lambda\beta^+ n_1\big(\beta_y^- n_1 n_2 - \beta_x^- n_2^2\big)\Big\}u_y^- \\ &\quad - \lambda\beta^-\beta^+ n_1^2 n_2 u_{xx}^- + \lambda\beta^-\beta^+ n_1\big(n_1^2 - n_2^2\big)u_{xy}^- + \lambda\beta^-\beta^+ n_1^2 n_2 u_{yy}^-. \end{aligned}$$

For brevity, u_x^+ and u_y^+ can be rewritten as

$$u_x^+ = \rho_2 u_x^- + \rho_3 u_y^- + \rho_4 u_{xx}^- + \rho_5 u_{xy}^- + \rho_6 u_{yy}^-, \tag{2.14}$$

where

$$\begin{aligned} \rho_2 &= \frac{\big(\beta^- n_1^2 + \beta^+ n_2^2\big)}{\beta^+} - \lambda\big(\beta_y^- n_1^2 n_2 - \beta_x^- n_1 n_2^2\big), \\ \rho_3 &= \frac{(\beta^- - \beta^+)n_1 n_2}{\beta^+} - \lambda\big(\beta_y^- n_1 n_2^2 - \beta_x^- n_2^3\big), \\ \rho_4 &= \lambda\beta^- n_1 n_2^2, \quad \rho_5 = -\lambda\beta^-\big(n_1^2 - n_2^2\big)n_2, \quad \rho_6 = -\lambda\beta^- n_1 n_2^2, \end{aligned}$$

and

$$u_y^+ = \sigma_2 u_x^- + \sigma_3 u_y^- + \sigma_4 u_{xx}^- + \sigma_5 u_{xy}^- + \sigma_6 u_{yy}^-, \tag{2.15}$$

where

$$\begin{aligned}
\sigma_2 &= \frac{(\beta^- - \beta^+)n_1 n_2}{\beta^+} + \lambda n_1\big(\beta_y^- n_1^2 - \beta_x^- n_1 n_2\big),\\
\sigma_3 &= \frac{\big(\beta^+ n_1^2 + \beta^- n_2^2\big)}{\beta^+} + \lambda n_1\big(\beta_y^- n_1 n_2 - \beta_x^- n_2^2\big),\\
\sigma_4 &= -\lambda\beta^- n_1^2 n_2, \quad \sigma_5 = \lambda\beta^- n_1\big(n_1^2 - n_2^2\big), \quad \sigma_6 = \lambda\beta^- n_1^2 n_2.
\end{aligned}$$

Taking partial derivatives of u_y^+ and u_x^+ in y yields

$$\begin{aligned}
u_{yy}^+ &= (\sigma_2)_y u_x^- + (\sigma_3)_y u_y^- + (\sigma_4)_y u_{xx}^- + \big(\sigma_2 + (\sigma_5)_y\big)u_{xy}^- + \big(\sigma_3 + (\sigma_6)_y\big)u_{yy}^-\\
&\quad + \sigma_4 u_{xxy}^- + \sigma_5 u_{xyy}^- + \sigma_6 u_{yyy}^-\\
&= \phi_2 u_x^- + \phi_3 u_y^- + \phi_4 u_{xx}^- + \phi_5 u_{xy}^- + \phi_6 u_{yy}^- + \phi_7 u_{xxy}^- + \phi_8 u_{xyy}^- + \phi_9 u_{yyy}^-, \qquad (2.16)\\
u_{xy}^+ &= (\rho_2)_y u_x^- + (\rho_3)_y u_y^- + (\rho_4)_y u_{xx}^- + \big(\rho_2 + (\rho_5)_y\big)u_{xy}^- + \big(\rho_3 + (\rho_6)_y\big)u_{yy}^-\\
&\quad + \rho_4 u_{xxy}^- + \rho_5 u_{xyy}^- + \rho_6 u_{yyy}^-\\
&= \psi_2 u_x^- + \psi_3 u_y^- + \psi_4 u_{xx}^- + \psi_5 u_{xy}^- + \psi_6 u_{yy}^- + \psi_7 u_{xxy}^- + \psi_8 u_{xyy}^- + \psi_9 u_{yyy}^-. \qquad (2.17)
\end{aligned}$$

According to the governing equation

$$\begin{aligned}
&-\beta_x^+ u_x^+ - \beta^+ u_{xx}^+ - \beta_y^+ u_y^+ - \beta^+ u_{yy}^+ + c^+ u^+ - f^+\\
&= -\beta_x^- u_x^- - \beta^- u_{xx}^- - \beta_y^- u_y^- - \beta^- u_{yy}^- + c^- u^- - f^-,
\end{aligned}$$

and so

$$\begin{aligned}
\beta^+ u_{xx}^+ &= \beta^- u_{xx}^- + \beta_x^- u_x^- - \beta_x^+ u_x^+ + \beta_y^- u_y^- - \beta_y^+ u_y^+\\
&\quad + \beta^- u_{yy}^- - \beta^+ u_{yy}^+ + c^+ u^+ - c^- u^- - [f].
\end{aligned}$$

Replacing the $u^+, u_x^+, u_y^+, u_{xy}^+, u_{yy}^+$ in above formula by (2.9) and (2.14)-(2.16), then $\beta^+ u_{xx}^+$ can be rewritten as

$$\begin{aligned}
u_{xx}^+ &= \theta_1 u^- + \theta_2 u_x^- + \theta_3 u_y^- + \theta_4 u_{xx}^- + \theta_5 u_{xy}^- + \theta_6 u_{yy}^-\\
&\quad + \theta_7 u_{xxy}^- + \theta_8 u_{xyy}^- + \theta_9 u_{yyy}^- - \frac{[f]}{\beta^+}, \qquad (2.18)
\end{aligned}$$

where

$$\begin{aligned}
\theta_1 &= \frac{[c]}{\beta^+}, \quad \theta_2 = \frac{(\beta_x^- - \beta_x^+\rho_2 - \beta_y^+\sigma_2 - \beta^+\phi_2 + \lambda c^+\beta^- n_1)}{\beta^+},\\
\theta_3 &= \frac{(\beta_y^- - \beta_x^+\rho_3 - \beta_y^+\sigma_3 - \beta^+\phi_3 + \lambda c^+\beta^- n_1)}{\beta^+},\\
\theta_4 &= \frac{(\beta^- - \beta_x^+\rho_4 - \beta_y^+\sigma_4 - \beta^+\phi_4)}{\beta^+}, \quad \theta_5 = -\frac{(\beta_x^+\rho_5 + \beta_y^+\sigma_5 + \beta^+\phi_5)}{\beta^+},\\
\theta_6 &= \frac{(\beta^- - \beta_x^+\rho_6 - \beta_y^+\sigma_6 - \beta^+\phi_6)}{\beta^+}, \quad \theta_7 = -\phi_7, \quad \theta_8 = -\phi_8, \quad \theta_9 = -\phi_9.
\end{aligned}$$

To develop a finite difference scheme for the irregular points, following the same approach as in the line shape interface. First, it should find the 7-point stencil of the irregular point (i, j), and then expand the 7 points $(u_{i+i_k,j+j_k})$ in the stencil by Taylor series about the interface point (x_i^*, y_j^*). In view of the interface curve is continuous and arbitrarily cut through the computational mesh, we flexibly choose the stencil points of the irregular point (x_i, y_j). The stencils for the irregular points is shown in Fig. 2.2. The stencil consists of 7 points, which including five standard points and two auxiliary points. The auxiliary points are flexible and choosing the closest points to the interface point (x_i^*, y_j^*). Using the superscript $-$ and $+$ to denote the limiting values of a function from one side or the other.

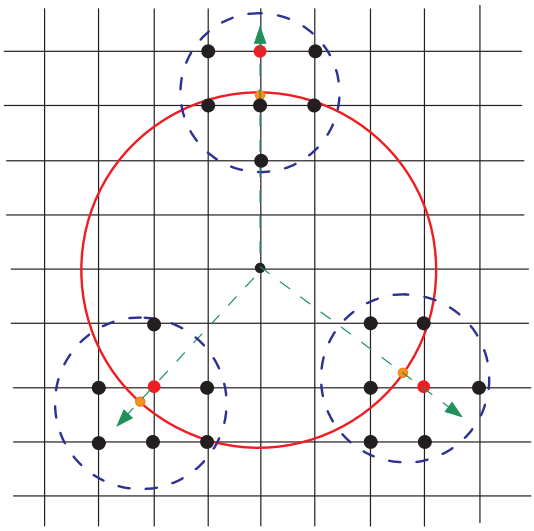

Fig. 2.2. The three kinds of stencils for the irregular point (k, j) for the curved interface.

When the point m in the stencil of irregular point (x_i, y_j) is located in Ω^-, the Taylor series of u_m at interface point (x_i^*, y_j^*) can be given as

$$\begin{aligned} u_m = u^- + h_{x,m}u_x^- + h_{y,m}u_y^- + \frac{h_{x,m}^2}{2}u_{xx}^- + \frac{h_{x,m}h_{y,m}}{2}u_{xy}^- \\ + \frac{h_{y,m}^2}{2}u_{yy}^- + \mathcal{O}(h^3), \quad m \in \Omega^-, \end{aligned} \tag{2.19}$$

where $h_{x,m} = x_m - \alpha$, $h_{y,m} = y_m - y_i$. For convenience of expression, it can be further written as

$$\begin{aligned} u_m = \omega_{m,1}u^- + \omega_{m,2}u_x^- + \omega_{m,3}u_y^- + \omega_{m,4}u_{xx}^- + \omega_{m,5}u_{xy}^- + \omega_{m,6}u_{yy}^- \\ + \omega_{m,7}u_{xxy}^- + \omega_{m,8}u_{xyy}^- + G_m + \mathcal{O}(h^3), \quad m \in \Omega^-, \end{aligned}$$

where

$$\begin{aligned} &\omega_{m,1} = 1, \qquad \omega_{m,2} = h_{x,m}, \qquad \omega_{m,3} = h_{y,m}, \\ &\omega_{m,4} = \frac{h_{x,m}^2}{2}, \quad \omega_{m,5} = \frac{h_{x,m}h_{y,m}}{2}, \quad \omega_{m,6} = \frac{h_{y,m}^2}{2}, \\ &\omega_{m,7} = \omega_{m,8} = \omega_{m,9} = G_m = 0. \end{aligned}$$

Similarly, when the point m in the stencil of irregular point (x_i, y_j) is locates in Ω^+, the Taylor series can be given as

$$u_m = u^+ + h_{x,m}u_x^+ + h_{y,m}u_y^+ + \frac{h_{x,m}^2}{2}u_{xx}^+ + \frac{h_{x,m}h_{y,m}}{2}u_{xy}^+ + \frac{h_{y,m}^2}{2}u_{yy}^+ + \mathcal{O}(h^3), \quad m \in \Omega^+. \tag{2.20}$$

Substitute the Eq. (2.9) and (2.14)-(2.18) into (2.20) and replace u^+, u_x^+, u_y^+, u_{xx}^+, u_{xy}^+ and u_{yy}^+, there is

$$u_m = \omega_{m,1}u^- + \omega_{m,2}u_x^- + \omega_{m,3}u_y^- + \omega_{m,4}u_{xx}^- + \omega_{m,5}u_{xy}^- + \omega_{m,6}u_{yy}^- + \omega_{m,7}u_{xxy}^- + \omega_{m,8}u_{xyy}^- + G_m + \mathcal{O}(h^3), \quad m \in \Omega^+, \tag{2.21}$$

where

$$\begin{aligned}
\omega_{m,1} &= 1 + \frac{h_{x,m}^2}{2}\theta_1,\\
\omega_{m,2} &= \lambda\beta^- n_1 + h_{x,m}\rho_2 + h_{y,m}\sigma_2 + \frac{h_{x,m}^2}{2}\theta_2 + \frac{h_{x,m}h_{y,m}}{2}\psi_2 + \frac{h_{y,m}^2}{2}\phi_2,\\
\omega_{m,3} &= \lambda\beta^- n_2 + h_{x,m}\rho_3 + h_{y,m}\sigma_3 + \frac{h_{x,m}^2}{2}\theta_3 + \frac{h_{x,m}h_{y,m}}{2}\psi_3 + \frac{h_{y,m}^2}{2}\phi_3,\\
\omega_{m,4} &= h_{x,m}\rho_4 + h_{y,m}\sigma_4 + \frac{h_{x,m}^2}{2}\theta_4 + \frac{h_{x,m}h_{y,m}}{2}\psi_4 + \frac{h_{y,m}^2}{2}\phi_4,\\
\omega_{m,5} &= h_{x,m}\rho_5 + h_{y,m}\sigma_5 + \frac{h_{x,m}^2}{2}\theta_5 + \frac{h_{x,m}h_{y,m}}{2}\psi_5 + \frac{h_{y,m}^2}{2}\phi_5,\\
\omega_{m,6} &= h_{x,m}\rho_6 + h_{y,m}\sigma_6 + \frac{h_{x,m}^2}{2}\theta_6 + \frac{h_{x,m}h_{y,m}}{2}\psi_6 + \frac{h_{y,m}^2}{2}\phi_6,\\
\omega_{m,7} &= \frac{h_{x,m}^2}{2}\theta_7 + \frac{h_{x,m}h_{y,m}}{2}\psi_7 + \frac{h_{y,m}^2}{2}\phi_7,\\
\omega_{m,8} &= \frac{h_{x,m}^2}{2}\theta_8 + \frac{h_{x,m}h_{y,m}}{2}\psi_8 + \frac{h_{y,m}^2}{2}\phi_8,\\
\omega_{m,9} &= \frac{h_{x,m}^2}{2}\theta_9 + \frac{h_{x,m}h_{y,m}}{2}\psi_9 + \frac{h_{y,m}^2}{2}\phi_9,\\
G_m &= -\frac{h_{x,m}^2}{2}\frac{[f]}{\beta^+}.
\end{aligned}$$

Suppose the seven points FD scheme of irregular point (x_i, y_j) is given in following form:

$$\gamma_1 u_1 + \gamma_2 u_2 + \gamma_3 u_3 + \gamma_4 u_4 + \gamma_5 u_5 + \gamma_6 u_6 + \gamma_7 u_7 + c_{k,j}u_{i,j}^h = f_{i,j} + R_{i,j}.$$

To require the truncation error being $\mathcal{O}(h)$, we get the following linear system with unknown $\gamma_s\,(1 \le s \le 7)$:

$$\begin{pmatrix}
\omega_{1,1} & \omega_{2,1} & \omega_{3,1} & \omega_{4,1} & \omega_{5,1} & \omega_{6,1} & \omega_{7,1}\\
\omega_{1,2} & \omega_{2,2} & \omega_{3,2} & \omega_{4,2} & \omega_{5,2} & \omega_{6,2} & \omega_{7,2}\\
\omega_{1,3} & \omega_{2,3} & \omega_{3,3} & \omega_{4,3} & \omega_{5,3} & \omega_{6,3} & \omega_{7,3}\\
\omega_{1,4} & \omega_{2,4} & \omega_{3,4} & \omega_{4,4} & \omega_{5,4} & \omega_{6,4} & \omega_{7,4}\\
\omega_{1,5} & \omega_{2,5} & \omega_{3,5} & \omega_{4,5} & \omega_{5,5} & \omega_{6,5} & \omega_{7,5}\\
\omega_{1,6} & \omega_{2,6} & \omega_{3,6} & \omega_{4,6} & \omega_{5,6} & \omega_{6,6} & \omega_{7,6}\\
\omega_{1,7} & \omega_{2,7} & \omega_{3,7} & \omega_{4,7} & \omega_{5,7} & \omega_{6,7} & \omega_{7,7}
\end{pmatrix}
\begin{pmatrix}\gamma_1\\ \gamma_2\\ \gamma_3\\ \gamma_4\\ \gamma_5\\ \gamma_6\\ \gamma_7\end{pmatrix}
=
\begin{pmatrix}0\\ -\beta_x^-\\ -\beta_y^-\\ -\beta^-\\ 0\\ -\beta^+\\ 0\end{pmatrix}, \tag{2.22}$$

and

$$R_{i,j} = -\sum_{p} \gamma_p \frac{h_{x,p}^2}{2} \frac{[f]}{\beta^+}, \quad p \in \{\Omega^+ \cap (1 \le p \le 7)\}.$$

3. Monotonicity, Stability and Convergence

Theorem 3.1. *The solution of two dimensional elliptic interface problems* (1.1) *with imperfect contact and the implicit jump conditions* (1.2)*, satisfies the maximum modulus estimation*

$$\|u\|_\infty \le \|g\|_\infty + C\|f\|_\infty,$$

where the constant C is a constant that depends on the spatial dimension and the diameter of the region Ω.

3.1. Stability

For the two dimensional elliptical interface problem (1.1) with imperfect contact and the implicit jump conditions (1.2), assume the reaction term $c(x, y) \ge 0$, then the unified finite difference scheme is

$$L_h u_{i,j}^h = \gamma_{i,j,0} u_{i,j,0}^h - \sum_{s=1}^{6} \gamma_{i,j,s} u_{i,j,s}^h = f_{i,j}, \tag{3.1}$$

where

$$u_{i,j,s}^h \begin{cases} = u_{i,j}^h, & s = 0, \\ \in \left\{ \begin{array}{cccc} u_{i,j}^h, & u_{i+1,j}^h, & u_{i,j-1}^h, & u_{i,j+1}^h, \\ u_{i-1,j-1}^h, & u_{i+1,j-1}^h, & u_{i-1,j+1}^h, & u_{i+1,j+1}^h \end{array} \right\}, & s = 1, 2, 3, 4, 5, 6, \end{cases}$$

and the number of points s as well as the coefficients γ for regular and irregular points are determined in above section. Notice that the local truncation error at the regular point is $T_{i,j} = \mathcal{O}(h^2)$, and the local truncation error at the non-regular point is $\tilde{T}_{i,j} = \mathcal{O}(h)$, where h is the grid size, $h = \text{diam}(\mathcal{T})$.

Theorem 3.2. *When the coefficient of the reaction term $c(x, y) \ge 0$ and the coefficient of the discrete format* (3.1) *meets the following conditions* [28]*:*

$$\gamma_{i,j,s} > 0, \quad \sum_{s=1}^{6} \gamma_{i,j,s} \le \gamma_{i,j,0},$$

the discrete format has the following estimate:

$$\|u^h\|_\infty \le \|g\|_\infty + C\|f_{i,j}\|_\infty.$$

3.2. Convergence analysis

Define $e_{i,j} = u_{i,j} - u_{i,j}^h$, the error equation is as follows:

$$L_h e_{i,j} = T_{i,j},$$

noticed that on the boundary $e_{i,j} = 0$.

Theorem 3.3. *When the coefficients of the reaction term $c(x,y) \geq 0$ and the coefficient of the discrete format* (3.1) *meet the following conditions:*

$$\gamma_{i,j,s} > 0, \quad \sum_{s=1}^{6} \gamma_{i,j,s} \leq \gamma_{i,j,0},$$

the error estimate of the numerical solution of the discrete format is as follows:

$$\|e_h\|_\infty \leq Ch.$$

Proof. According to the construction process of the finite difference scheme

$$\|T_{i,j}\|_\infty < Ch^2, \quad \|\tilde{T}\|_\infty < Ch.$$

Applying the stability theorem to the error equation, then

$$\|e_h\|_\infty \leq C \max\left\{\|T_{i,j}\|_\infty, \|\tilde{T}\|_\infty\right\} \leq Ch.$$

The proof is complete. □

3.3. Monotonicity

Theorem 3.4. *Assume the elliptic problems* (1.1), (1.2) *satisfy $u \in C^1(\overline{\Omega^\pm} \cup \Gamma) \cap C^2(\Omega^\pm \cup \Gamma)$, $c \in C(\overline{\Omega^+} \cup \overline{\Omega^-})$ and the interface Γ is smooth* [5]. *Let $c \geq 0, \lambda > 0, f \geq 0$ and $g \geq 0$, then $u \geq 0$ in Ω.*

Theorem 3.4 states that the solution of elliptic problems (1.1) with imperfect contact and jumping connecting condition (1.2) is positivity-preserving. We will analysis the presented scheme is monotone in particular case, where the interface is straight, and the diffusion coefficient is constant, etc.

When the interface is straight, the diffusion coefficient β is constant and the coefficient of the reaction term $c(x,y) = 0, \lambda > 0$, the linear system (2.6) at the irregular point (x_k, y_j) can be rewritten as

$$\mathbf{H}\gamma = \mathbf{b}, \tag{3.2}$$

where

$$\mathbf{H} = \begin{pmatrix} 1 & 1 & 1 & 1 & 1 & 1 & 1 \\ h_{x,1} & h_{x,2} & h_{x,2} & h_{x,2} & \chi_1 & \chi_1 & \chi_1 \\ 0 & -1 & 0 & 1 & -1 & 0 & 1 \\ h_{x,1}^2 & h_{x,2}^2 & h_{x,2}^2 & h_{x,2}^2 & \chi_2 & \chi_2 & \chi_2 \\ 0 & -h_{x,2} & 0 & h_{x,2} & -\chi_1 & 0 & \chi_1 \\ 0 & h^2 & 0 & h^2 & h^2 - \chi_3 & -\chi_3 & h^2 - \chi_3 \\ 0 & 0 & 0 & 0 & h^2 - h_{x,5}^2 & -h_{x,5}^2 & h^2 - h_{x,5}^2 \end{pmatrix},$$

$$\gamma = [\gamma_1, \gamma_2, \gamma_3, \gamma_4, \gamma_5, \gamma_6, \gamma_7]^T, \quad \mathbf{b} = [0, 0, 0, -2\beta^-, 0, -2\beta^+, 0]^T,$$

and

$$\chi_1 = \lambda\beta^- + \frac{\beta^-}{\beta^+} h_{x,5}, \quad \chi_2 = \frac{\beta^-}{\beta^+} h_{x,5}^2, \quad \chi_3 = \frac{[\beta]}{\beta^+} h_{x,5}^2.$$

Solve the above linear system (3.2), there is

$$\gamma_i = \frac{D_i}{D}, \quad i = 1, 2, \ldots, 7,$$

where

$$D = \lambda\beta^-(h_{x,1} + h_{x,2}) - h_{x,1}h_{x,2} + \frac{\beta^-}{\beta^+}(h_{x,1} + h_{x,2} - h_{x,5}),$$
$$D_1 = \frac{2\beta^-}{h}\left(\lambda\beta^- + \frac{\beta^-}{\beta^+}h_{x,5} - h_{x,2}\right),$$
$$D_2 = D_4 = \left(2h^2\left(-2\beta^-(h_{x,1} + h_{x,2})(\lambda\beta^+ + h_{x,5}) + 2\beta^+h_{x,1}h_{x,2} + 2\frac{\beta^-}{\beta^+}[\beta]h_{x,5}^2\right)\right)^{-1},$$
$$D_3 = -\frac{1}{h^3}\left(\frac{\beta^-[\beta]}{\beta^+}hh_{x,5}^2 + \frac{2\beta^-}{\beta^+}h^2h_{x,5} + 2\beta^+hh_{x,1}h_{x,2} - 2\lambda\beta^-\beta^+h(h_{x,1} + h_{x,2}) + 2\lambda\beta^{-^2}h^2\right),$$
$$D_5 = D_7 = \frac{1}{4h^2h_{x,5}^2\beta^-}, \quad D_6 = \frac{2\beta^-(h^2 - h_{x,5}^2)}{h^2}.$$

Noticing, $h_{x,1} < 0$, $h_{x,2} < 0$, $h_{x,5} > 0$, $\beta^- > 0$, $\beta^+ > 0$, $[\beta] > 0$, then $D < 0, D_1 > 0$, $D_2 = D_4 > 0, D_3 < 0, D_5 = D_7 > 0$. Thus, we can get that

$$\gamma_1 < 0, \quad \gamma_2 = \gamma_4 < 0, \quad \gamma_3 > 0, \quad \gamma_5 = \gamma_7 < 0.$$

Similarly, when the diffusion coefficient β is constant and the coefficient of the reaction term $c(x, y) = 0$, the linear system (2.8) of the irregular point (x_{k+1}, y_j) can be rewritten as

$$\bar{\mathbf{H}}\bar{\gamma} = \mathbf{b}, \tag{3.3}$$

where

$$\bar{\mathbf{H}} = \begin{pmatrix} 1 & 1 & 1 & 1 & 1 & 1 & 1 \\ h_{x,1} & h_{x,2} & h_{x,2} & h_{x,2} & \bar{\chi}_1 & \bar{\chi}_1 & \bar{\chi}_1 \\ 0 & -1 & 0 & 1 & -1 & 0 & 1 \\ h_{x,1}^2 & h_{x,2}^2 & h_{x,2}^2 & h_{x,2}^2 & \bar{\chi}_2 & \bar{\chi}_2 & \bar{\chi}_2 \\ 0 & -h_{x,2} & 0 & h_{x,2} & -\bar{\chi}_1 & 0 & \bar{\chi}_1 \\ 0 & h^2 & 0 & h^2 & h^2 - \bar{\chi}_3 & -\bar{\chi}_3 & h^2 - \bar{\chi}_3 \\ 0 & 0 & 0 & 0 & h^2 - h_{x,5}^2 & -h_{x,5}^2 & h^2 - h_{x,5}^2 \end{pmatrix},$$

$$\bar{\gamma} = [\bar{\gamma}_1, \bar{\gamma}_2, \bar{\gamma}_3, \bar{\gamma}_4, \bar{\gamma}_5, \bar{\gamma}_6, \bar{\gamma}_7]^T,$$

and

$$\bar{\chi}_1 = -\lambda\beta^+ + \frac{\beta^+}{\beta^-}h_{x,5}, \quad \bar{\chi}_2 = -\frac{\beta^+}{\beta^-}h_{x,5}^2, \quad \bar{\chi}_3 = \frac{[\beta]}{\beta^-}h_{x,5}^2.$$

Solve the above linear system (3.3), there is

$$\bar{\gamma}_i = \frac{\bar{D}_i}{\bar{D}}, \quad i = 1, 2, \ldots, 7,$$

where

$$\bar{D} = -\lambda\beta^+(h_{x,1} + h_{x,2}) - h_{x,1}h_{x,2} + \frac{\beta^+}{\beta^-}h_{x,5}(h_{x,1} + h_{x,2} + h_{x,5}),$$

$$\bar{D}_1 = \frac{1}{h}\left(2\lambda\beta^-\beta^+ - 2\beta^+ h_{x,5} + 2\beta^- h_{x,2}\right),$$

$$\bar{D}_2 = \bar{D}_4 = \left(2h^2\left(2\lambda{\beta^+}^2(h_{x,1}+h_{x,2}) + 2\beta^+(h_{x,1}h_{x,2} - h_{x,5}^2) - 2\frac{{\beta^+}^2}{\beta^-}h_{x,5}(h_{x,1}+h_{x,2}+h_{x,5})\right)\right)^{-1},$$

$$\bar{D}_3 = \frac{1}{h^3}\Big(- 2\beta^- h^2(\lambda\beta^+ + h_{x,1}) - 2\beta^+ h h_{x,1}h_{x,2} + 2\beta^+ h h_{x,5}(h - h_{x,5})$$
$$- 2\lambda\beta^-\beta^+ h(h_{x,1} + h_{x,2}) + 2\frac{{\beta^+}^2}{\beta^-}h h_{x,5}(h_{x,1} + h_{x,2} - h_{x,5})\Big),$$

$$\bar{D}_5 = \bar{D}_7 = \frac{1}{4h^2 h_{x,5}^2\beta^-}, \quad \bar{D}_6 = \frac{2\beta^-(h^2 - h_{x,5}^2)}{h^2}.$$

Owing to $h_{x,1} > 0$, $h_{x,2} > 0$, $h_{x,5} < 0$, $\beta^- > 0$, $\beta^+ > 0$, $[\beta] > 0$, then $\bar{D} < 0, \bar{D}_1 > 0$, $\bar{D}_2 = \bar{D}_4 > 0, \bar{D}_3 < 0, \bar{D}_5 = \bar{D}_7 > 0$. Thus, we can get that

$$\bar{\gamma}_1 < 0, \quad \bar{\gamma}_2 = \bar{\gamma}_4 < 0, \quad \bar{\gamma}_3 > 0, \quad \bar{\gamma}_5 = \bar{\gamma}_7 < 0.$$

Theorem 3.5. *For the elliptic problems* (1.1) *with imperfect contact* (1.2) *and the interface is straight. Let β is contact, $c \geq 0, \lambda > 0, f \geq 0$ and $g \geq 0$, the linear algebraic system $(AX = b)$ resulted from the difference scheme satisfying $a_{ii}>0$ $(1 \leq i \leq n)$ and $a_{ij}\leq 0$ $(1 \leq i, j \leq n, i \neq j)$. Then matrix A is M matrix and the scheme is monotone.*

Proof. From the above analysis, it is clear that the matrix $A = (a_{ij})_{n\times n}$ satisfying $a_{ii} > 0$ $(1 \leq i \leq n)$ and $a_{ij} \leq 0$ $(1 \leq i, j \leq n, i \neq j)$, when β is contact, $c \geq 0, \lambda > 0, f \geq 0$ and $g \geq 0$. Considering the matrix A is reversible, thus it is a M-matrix. We can prove that our new scheme is monotone, more details can be refereed in [38]. □

4. Numerical Experiments

In this section, we use several numerical experiments to demonstrate the performance of the discrete schemes.

Example 4.1. Consider the two-dimensional problem with computational domain $\Omega = [0, 1] \times [0, 1]$, and the solution separated into two parts by the interface at $x = \alpha$, $\alpha = 0.534$, as shown in Fig. 4.1. The analytical solution of this problem is given by

$$u(x, y) = \begin{cases} e^x \cos my, & (x, y) \in (0, \alpha) \times [0, 1], \\ \kappa e^x \cos my, & (x, y) \in (\alpha, 1) \times [0, 1]. \end{cases}$$

The diffusion coefficient is defined as follows:

$$\beta = \begin{cases} \kappa, & (x, y) \in (0, \alpha) \times [0, 1], \\ 1, & (x, y) \in (\alpha, 1) \times [0, 1]. \end{cases}$$

The conservation of the flux on interface is satisfied

$$\left[\beta\frac{\partial u}{\partial x}\right] = \beta^+\frac{\partial u^+}{\partial x} - \beta^-\frac{\partial u^-}{\partial x} = \kappa e^x \cos 3y - \kappa e^x \cos 3y = 0 \quad \text{on } \Gamma.$$

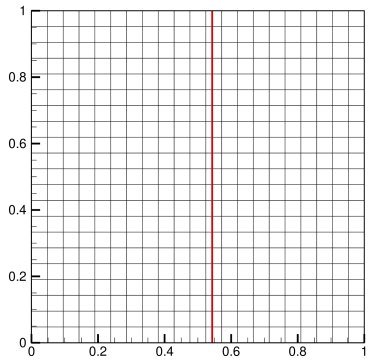

Fig. 4.1. The computational mesh.

The coefficient λ is given as

$$\lambda = \frac{1-\kappa}{\kappa}.$$

Tables 4.1 and 4.2 give the L_2 and L_∞ errors and convergence rate under different grid numbers at $\kappa = 2, 10, 100$ and $\kappa = 1000$, respectively. From these tables it can be seen that the L_2 and L_∞ errors are decreasing as the number of cells increased. The convergence rate of the two kinds of errors is approximate to second-order accuracy.

Fig. 4.2 shows the surface and contour of numerical solution with the cells number is 40×40 at $\kappa = 100$. There is a sharp jump along both sides of material interface. The presented numerical scheme is able to capture the discontinuity of solution and achieve sufficient accuracy.

Fig. 4.3 compares errors of the numerical solutions at different ratio of diffusion coefficient $\kappa = 10$ and $\kappa = 1000$. We can see that the errors of the numerical solution increases with the increase of the diffusion coefficient ratio κ.

Table 4.1: The comparison of L_2 and L_∞ errors by present FDM scheme at $\kappa = 2, 10$, Example 4.1.

Mesh	κ=2				κ=10			
	L_2	Rate	L_∞	Rate	L_2	Rate	L_∞	Rate
21×21	7.84e-3		2.58e-2		6.72e-3		1.44e-2	
41×41	2.14e-3	1.87	9.57e-3	1.48	2.10e-3	1.83	4.40e-3	1.71
81×81	6.38e-4	1.75	3.30e-3	1.54	5.21e-4	2.01	1.38e-3	1.67
161×161	1.70e-4	1.91	9.01e-4	1.87	1.31e-4	1.98	4.13e-4	1.74
321×321	4.74e-5	1.84	2.40e-4	1.91	3.60e-5	1.86	1.46e-4	1.53

Table 4.2: The comparison of L_2 and L_∞ errors by present FDM scheme at $\kappa = 100, 1000$, Example 4.1.

Mesh	κ=100				κ=1000			
	L_2	Rate	L_∞	Rate	L_2	Rate	L_∞	Rate
41×41	6.66e-3		1.84e-2		6.29e-2		1.54e-1	
81×81	1.68e-3	1.99	4.88e-3	1.91	1.52e-2	2.05	3.77e-2	2.03
161×161	4.83e-4	1.80	1.47e-3	1.73	4.05e-3	1.81	1.11e-2	1.76
321×321	1.16e-4	2.05	3.69e-4	1.99	9.51e-4	2.09	2.73e-3	2.02

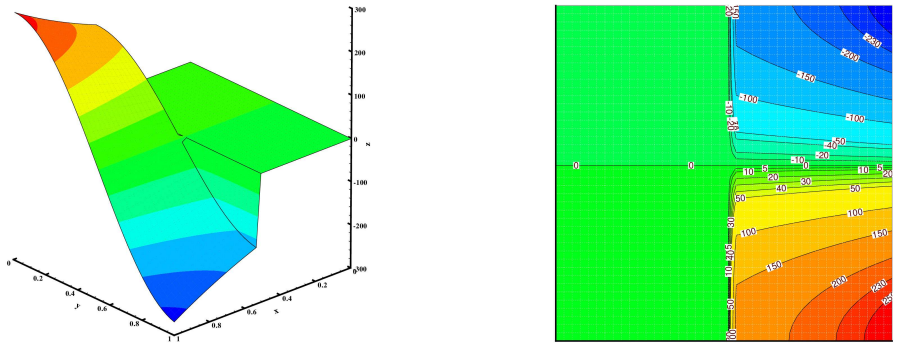

(a) Surface (b) Contour

Fig. 4.2. The surface and contour for Example 4.1 with $\kappa = 100$, the number of cells is 40×40.

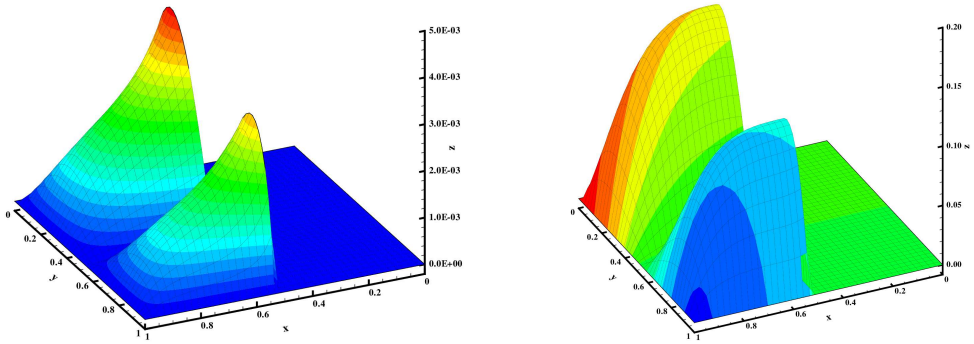

(a) $\kappa = 10$ (b) $\kappa = 1000$

Fig. 4.3. The errors of Example 4.1 with $\kappa = 10, 1000$, the number of cells is 40×40.

Example 4.2. Consider the computational domain $\Omega = [0,1] \times [0,1]$, and the solution is separated into two parts by the interface at $x = 0.5$. The analytical solution of this problem is given by

$$u(x,y) = \begin{cases} x + \sin y, & (x,y) \in (0,\alpha) \times [0,1], \\ \kappa(x + \sin y), & (x,y) \in (\alpha,1) \times [0,1]. \end{cases}$$

The diffusion coefficient is defined as follows:

$$\beta(x,y) = \begin{cases} \kappa, & (x,y) \in (0,\alpha) \times [0,1], \\ 1, & (x,y) \in (\alpha,1) \times [0,1]. \end{cases}$$

The conservation of the flux at interface is satisfied

$$\left[\kappa \frac{\partial u}{\partial \vec{n}}\right] = \kappa^+ \frac{\partial u^+}{\partial \vec{n^-}} - \kappa^- \frac{\partial u^-}{\partial \vec{n^-}} = 0 \quad \text{on } \Gamma.$$

The coefficient λ in (1.2) is given as

$$\lambda = \frac{\kappa - 1}{\kappa} \left(\frac{1}{2} + \sin y\right).$$

Tables 4.3 and 4.4 compare the L_2 and L_∞ errors between the present finite difference method and the monotone finite volume method in [5]. We can see that the L_2 and L_∞ errors decrease as the number of cells increase and the convergence rate is almost achieve second-order accuracy. However, the errors of the presented FDM is larger than that in [5] under the same grid number.

Fig. 4.4 shows the surface and contour of numerical solution with the cells number is 40×40 $\kappa = 10$. The errors with $\kappa = 100$ is shown in Fig. 4.5.

Table 4.3: The comparison of L_2 and L_∞ errors by present FDM scheme and monotone FVM in [5] for Example 4.2, k=10.

Mesh	Present FDM				Monotone FVM [5]			
	L_2	Rate	L_∞	Rate	L_2	Rate	L_∞	Rate
13×13	6.58e-2		1.90e-1		1.73e-3		6.59e-3	
25×25	1.94e-2	1.76	5.25e-2	1.86	4.43e-4	1.97	2.10e-3	1.65
49×49	4.93e-3	1.97	1.45e-2	1.85	1.13e-4	1.97	6.27e-4	1.74
97×97	1.36e-3	1.86	3.52e-3	2.04	2.92e-5	1.95	1.62e-4	1.96
193×193	4.20e-4	1.70	9.84e-4	1.84	7.17e-6	2.02	4.44e-5	1.87
385×385	1.20e-4	1.81	2.67e-4	1.88	1.78e-6	2.01	1.20e-5	1.90

Table 4.4: The comparison of L_2 and L_∞ errors by present FDM scheme and monotone FVM in [5] for Example 4.2, k=100.

Mesh	Present FDM				Monotone FVM [5]			
	L_2	Rate	L_∞	Rate	L_2	Rate	L_∞	Rate
13×13	6.81e-1		1.696		1.72e-2		6.58e-2	
25×25	2.07e-1	1.71	4.92e-1	1.78	4.40e-3	1.97	2.10e-2	1.65
49×49	5.42e-2	1.93	1.44e-1	1.77	1.12e-3	1.97	6.27e-3	1.74
97×97	1.45e-2	1.90	4.33e-2	1.73	2.89e-4	1.95	1.61e-3	1.96
193×193	4.23e-3	1.78	1.60e-2	1.45	7.10e-5	2.02	4.44e-4	1.86
385×385	1.30e-3	1.71	4.31e-3	1.89	1.80e-5	1.98	1.20e-4	1.90

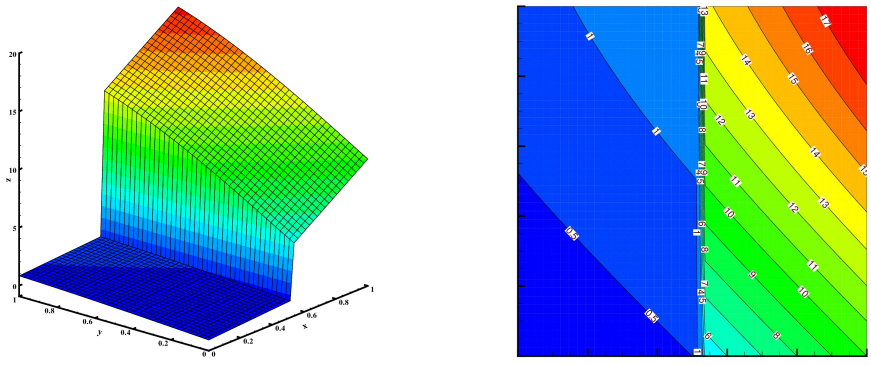

(a) Surface (b) Contour

Fig. 4.4. The surface and contour of numerical solutions for Example 4.2 with $\kappa = 10$, the number of cells is 40×40.

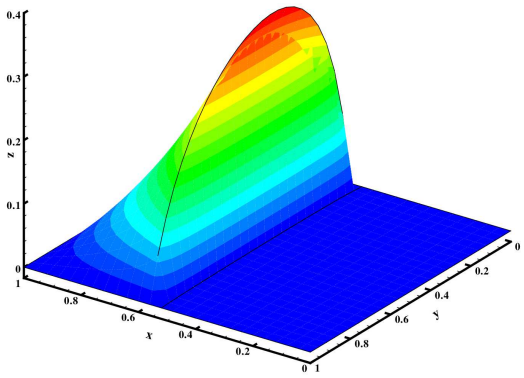

Fig. 4.5. The errors for Example 4.2 with $\kappa = 100$, the number of cells is 40×40.

Example 4.3. Consider the two dimensional problem with curved interface in computational domain $\Omega = [0, 1] \times [0, 1]$, and the solution is separated into two parts by the interface. The analytical solution of this problem is given by

$$u(x, y) = \begin{cases} \dfrac{x^2 + y^2}{\kappa} + 1.0, & x^2 + y^2 \leq 0.5^2, \\ x^2 + y^2, & \text{otherwise.} \end{cases}$$

The diffusion coefficient is defined as follows:

$$\beta = \begin{cases} \kappa, & x^2 + y^2 \leq 0.5^2, \\ 1, & \text{otherwise.} \end{cases}$$

The conservation of the flux on interface is satisfied

$$\left[\beta \frac{\partial u}{\partial x}\right] = \beta^+ \frac{\partial u^+}{\partial x} - \beta^- \frac{\partial u^-}{\partial x} = 0 \quad \text{on } \Gamma.$$

The coefficient λ in this test case is

$$\lambda = \frac{-(3\kappa + 1)}{4\kappa}.$$

Tables 4.5 and 4.6 compare the L_2 and L_∞ errors and convergence rate by present FDM scheme and monotone FVM in [5], under different grid numbers for $\kappa = 2, 100$, respectively. It

Table 4.5: The comparison of L_2 and L_∞ errors by present FDM scheme and monotone FVM in [5] for Example 4.3, κ=2.

Mesh	Present FDM				Cells	Monotone FVM [5]			
	L_2	Rate	L_∞	Rate		L_2	Rate	L_∞	Rate
41×41	1.88e-4		4.33e-4		262	2.09e-1		5.77e-1	
81×81	4.61e-5	2.02	1.10e-4	1.97	1234	5.27e-2	1.98	2.97e-1	0.96
161×161	1.29e-5	1.85	2.86e-5	1.94	2738	1.28e-2	2.03	1.46e-1	1.02
321×321	2.97e-6	2.11	7.25e-6	1.98	4862	3.21e-3	1.99	7.43e-2	0.97

Table 4.6: The comparison of L_2 and L_∞ errors by present FDM scheme and monotone FVM in [5] for Example 4.3, κ=100.

Mesh	Present FDM				Cells	Monotone FVM [5]			
	L_2	Rate	L_∞	Rate		L_2	Rate	L_∞	Rate
41×41	5.40e-3		8.82e-3		262	2.09e-1		5.77e-1	
81×81	1.09e-3	2.30	1.86e-3	2.25	1234	5.27e-2	1.98	2.97e-1	0.96
161×161	2.62e-4	2.06	4.67e-4	1.99	2738	1.28e-2	2.03	1.46e-1	1.02
321×321	6.87e-5	1.93	1.19e-4	1.97	4862	3.21e-3	1.99	7.43e-2	0.97

Table 4.7: The L_2 and L_∞ errors for Example 4.3, κ=1000.

Error / Mesh	L_2^u	Rate	L_∞^u	Rate
21×21	1.75e-1		2.72e-1	
41×41	5.35e-2	1.71	8.80e-2	1.63
81×81	1.07e-2	2.32	1.84e-2	2.26
161×161	2.64e-3	2.02	4.76e-3	1.95
321×321	6.63e-4	1.99	1.15e-3	2.05

can be seen that the convergent rate of the two kinds of errors is about second order. In this test example, the computational errors of the presented FDM is much smaller than the monotone FVM method in [5]. This means that the presented method can achieve more accurate numerical results.

Table 4.7 presents the L_2 and L_∞ errors and convergence rate for $\kappa = 1000$. It can be seen that when the ratio of diffusion coefficients κ on both sides of the interface is large, the convergence rate of the numerical scheme can still maintain approximate second-order accuracy.

Fig. 4.6 shows the non-body fitted computational mesh with circular interface.

Fig. 4.7 displays the surface and contour of numerical solution for Example 4.3 with 40×40 cells.

Fig. 4.8 gives the errors of Example 4.3 with $\kappa = 10$ and $\kappa = 1000$, respectively.

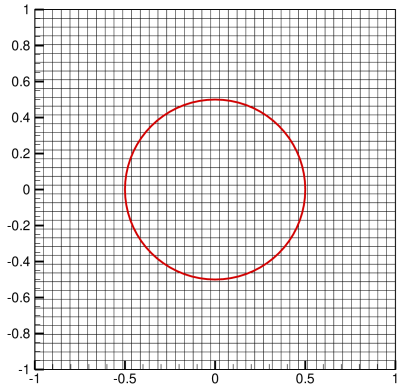

Fig. 4.6. The computational mesh.

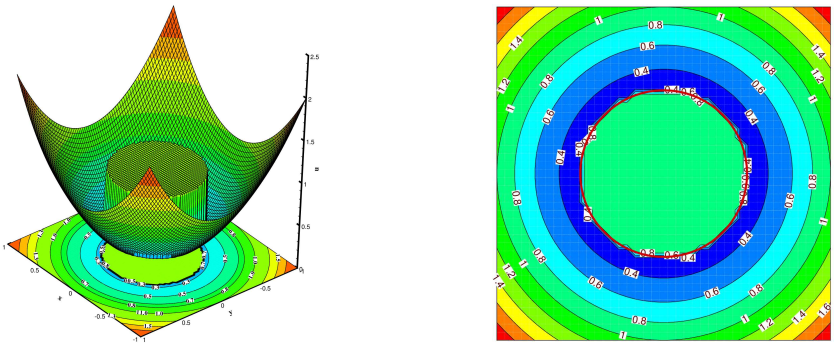

(a) Surface (b) Contour

Fig. 4.7. The surface and contour under 40×40 cells for Example 4.3 with $\kappa = 10$.

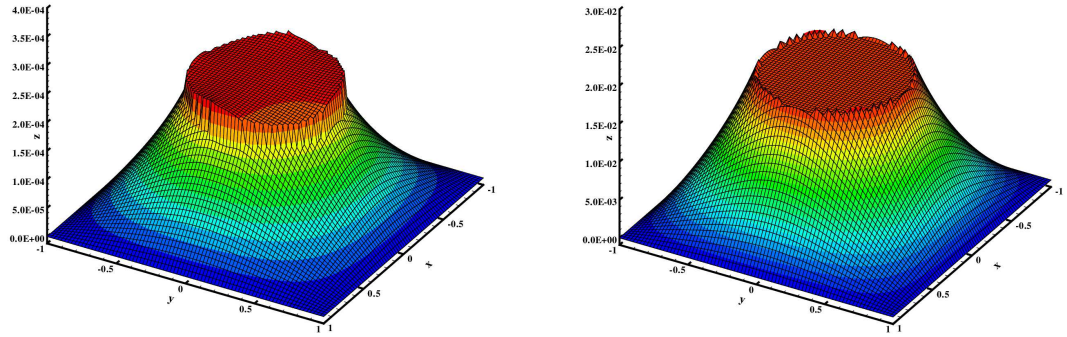

(a) $\kappa = 10$ (b) $\kappa = 1000$

Fig. 4.8. The errors for Example 4.3 with $\kappa = 10, 1000$, the number of cells is 80×80.

Example 4.4. In this case, we exchange the two sub-zones Ω^- and Ω^+, i.e.

$$\Omega^+ = \{(x, y)|x^2 + y^2 \leq 0.5^2)\}, \quad \Omega^- = \Omega \setminus \Omega^+.$$

The computational zone, the analytic solution, the location of interface and other parameters are the same as those in Example 4.3.

Table 4.8 presents the L_2 and L_∞ errors and convergence rate of the presented FDM and the monotone FVM in [5]. It can be seen that the results of the both methods can be approximated to second-order accuracy. Meanwhile, the numerical errors of the presented method is far smaller than that of the FVM method, and a better accuracy is achieved.

Table 4.8: The comparison of L_2 and L_∞ errors by present FDM scheme and monotone FVM in [5] for Example 4.4, κ=100.

Mesh	Present FDM				Cells	Monotone FVM [5]			
	L_2	Rate	L_∞	Rate		L_2	Rate	L_∞	Rate
41×41	3.38e-5		9.96e-5		262	2.09e-1		5.77e-1	
81×81	1.09e-5	1.63	3.20e-5	1.64	1234	5.27e-2	1.98	2.97e-1	0.96
161×161	2.61e-6	2.06	7.52e-6	2.09	2738	1.28e-2	2.03	1.46e-1	1.02
321×321	6.82e-7	1.96	1.92e-6	1.97	4862	3.21e-3	1.99	7.43e-2	0.97

Table 4.9 displays the L_2 and L_∞ errors and convergence rate for κ=1000. It can be seen that when the κ is large, the numerical result is still relatively stable, and it can approximately achieve second-order accuracy.

Fig. 4.9 displays the surface and contour of the numerical solution with $\kappa = 100$ for Example 4.4.

Fig. 4.10 gives errors of Example 4.4 with $\kappa = 2$. It can be seen that the calculation error decreases significantly as the number of cells is increased.

Table 4.9: The L_2 and L_∞ errors for Example 4.4, κ=1000.

Error / Mesh	L_2^u	Rate	L_∞^u	Rate
21×21	1.66e-4		5.27e-4	
41×41	4.32e-5	1.94	1.40e-4	1.91
81×81	1.07e-5	2.01	3.22e-5	2.12
161×161	2.56e-6	2.06	7.33e-6	2.13
321×321	6.88e-7	1.90	1.96e-6	1.90

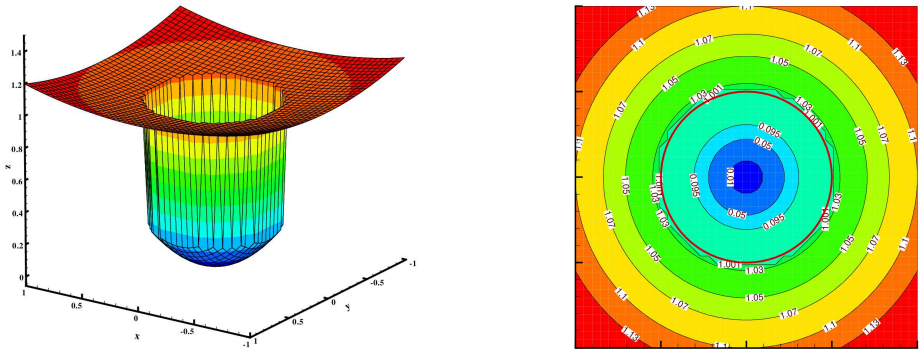

(a) Surface (b) Contour

Fig. 4.9. The surface and contour of Example 4.4 with $\kappa = 100$, the number of cells is 40×40.

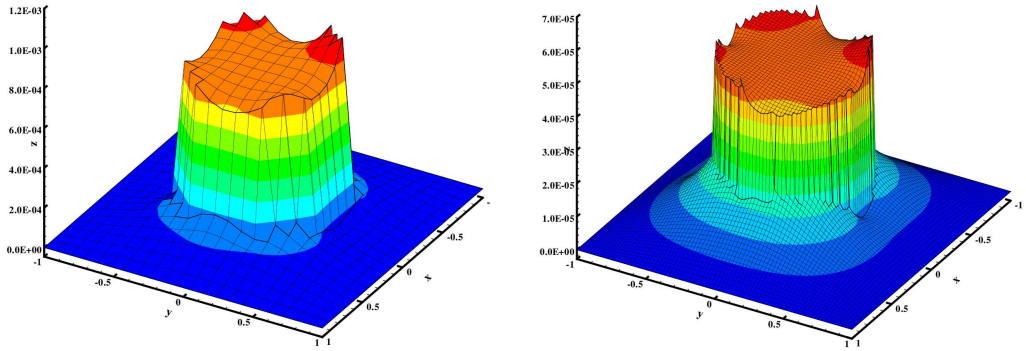

(a) 21×21 (b) 81×81

Fig. 4.10. The errors of Example 4.4 with $\kappa = 2$ on different number of cells.

Example 4.5. Consider the two dimensional problem in computational domain $\Omega = [-1, 1] \times [-1, 1]$, and the solution is separated in two parts by curve interface. The analytical solution of this problem is given by

$$u(x, y) = \begin{cases} \dfrac{\sin(x^2 + y^2)}{\kappa} + 1.0, & x^2 + y^2 \leq 0.5^2, \\ \sin(x^2 + y^2), & \text{otherwise.} \end{cases}$$

The diffusion coefficient is defined as follows:

$$\beta = \begin{cases} \kappa, & x^2 + y^2 \leq 0.5^2, \\ 1, & \text{otherwise.} \end{cases}$$

The conservation of the flux on interface is satisfied

$$\left[\beta \frac{\partial u}{\partial x}\right] = \beta^+ \frac{\partial u^+}{\partial x} - \beta^- \frac{\partial u^-}{\partial x} = 0 \quad \text{on } \Gamma.$$

The coefficient λ in this case is

$$\lambda = \frac{(\kappa - 1)\sin(1/4) - \kappa}{\kappa \cos(1/4)}.$$

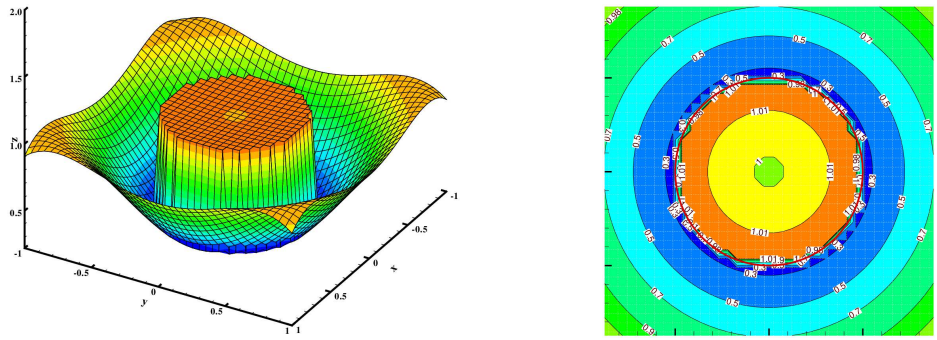

(a) Surface (b) Contour

Fig. 4.11. The surface and contour of Example 4.5 with $\kappa = 10$, the number of cells is 40×40.

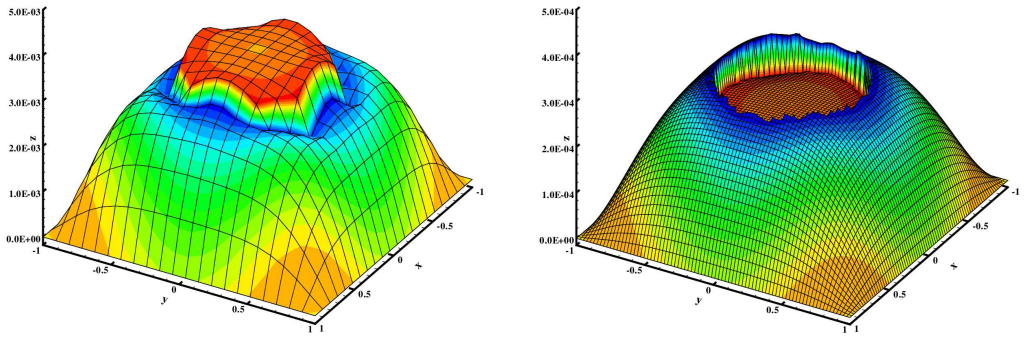

(a) 21×21 (b) 81×81

Fig. 4.12. The errors for Example 4.5 with $\kappa = 2$ on different mesh.

Table 4.10: The comparison of L_2 and L_∞ errors by present FDM scheme of Example 4.5 at $\kappa = 10, 100$.

Mesh	κ=10				κ=100			
	L_2	Rate	L_∞	Rate	L_2	Rate	L_∞	Rate
21×21	2.08e-3		2.92e-3		2.00e-3		2.78e-3	
41×41	5.38e-4	1.95	7.52e-4	1.96	5.21e-4	1.94	7.33e-4	1.92
81×81	1.42e-4	1.92	2.13e-4	1.82	1.68e-4	1.82	2.09e-4	1.81
161×161	3.76e-5	1.92	4.71e-5	2.11	4.25e-5	1.80	4.28e-5	2.12
321×321	1.03e-5	1.87	1.58e-5	1.83	1.00e-5	2.08	1.22e-5	1.81

Table 4.10 shows the L_2 and L_∞ errors and convergence rate for $\kappa = 10, 100$. It can be seen that the error decreases as the number of cells increased. For different κ value, the convergence rates can be approximated to second-order accuracy.

Fig. 4.11 presents the surface and contour of the numerical solution for Example 4.5 with $\kappa = 10$, the number of cells is 40×40.

Fig. 4.12 gives errors under different number of grids for Example 4.5 with $\kappa = 2$. It can be seen that the computational error decreases significantly as the number of grids is increased.

5. Conclusion

A finite difference method for 2D elliptic interface equations with imperfect contact is presented. The key feature of the imperfect connection condition is that the jump qualities of the solution is unknown and related with the flux across the interface. For the shapes of the straight and curved interface, an efficient finite difference method is constructed. The stability and convergence property is analyzed for the schemes of 2D linear problems. Further, the monotonicity of the scheme is proved in particular case. Numerical results show that the presented scheme approximately achieves second-order accuracy.

Acknowledgments. This work is partially supported by the National Natural Science Foundation of China (Grants 12261067, 12161067, 12361088, 62201298, 12001015, 51961031), by the Inner Mongolia Autonomous Region "Youth Science and Technology Talents" support program (Grant NJYT20B15), by the Inner Mongolia Scientific Fund Project (Grants 2020MS06010, 2021LHMS01006, 2022MS01008) and by the Innovation fund project of Inner Mongolia University of science and technology-Excellent Youth Science Fund Project (Grant 2019YQL02).

References

[1] J.R. Babber and R. Zhang, Transient behaviour and stability for the thermoelastic contact of the rods of dissimilar materials, *Int. J. Mech. Sci.*, **30** (1988), 691–704.

[2] J.W. Barrett and C.M. Elliott, Fitted and unfitted finite-element methods for elliptic equations with smooth interfaces, *IMA J. Numer. Anal.*, **7** (1987), 283–300.

[3] D. Bochkov and F. Gibou, Solving elliptic interface problems with jump conditions on Cartesian grids, *J. Comput. Phys.*, **407** (2020), 109269.

[4] E. Burman and A. Ern, An unfitted Hybrid High-Order method for elliptic interface problems, *SIAM J. Numer. Anal.*, **56**:3 (2018), 1525–1546.

[5] F. Cao, Z. Sheng, and G. Yuan, Monotone finite volume schemes for diffusion equation with imperfect interface on distorted meshes, *J. Sci. Comput.*, **76**:2 (2018), 1055–1077.

[6] W. Cao, X. Zhang, Z. Zhang, and Q. Zou, Superconvergence of immersed finite volume methods for one-dimensional interface problems, *J. Sci. Comput.*, **73**:2–3 (2017), 543–565.
[7] Y. Chen, S. Hou, and X. Zhang, An immersed finite element method for elliptic interface problems with multi-domain and triple junction points, *Adv. Appl. Math. Mech.*, **11**:5 (2019), 1005–1021.
[8] A. Coco and G. Russo, Second order finite-difference ghost-point multigrid methods for elliptic problems with discontinuous coefficients on an arbitrary interface, *J. Comput. Phys.*, **361** (2018), 299–330.
[9] R. Costa, J.M. Nobrega, S. Clain, and G.J. Machado, Very high-order accurate polygonal mesh finite volume scheme for conjugate heat transfer problems with curved interfaces and imperfect contacts, *Comput. Methods Appl. Mech. Engrg.*, **357** (2019), 112560.
[10] P. Donato and S. Monsurro, Homogenization of two heat conductors with an interfacial contact resistance, *Anal. Appl.*, **2**:3 (2004), 47–273.
[11] H. Guo and X. Yang, Gradient recovery for elliptic interface problem: I. Body-fitted mesh, *Commun. Comput. Phys.*, **23**:5 (2018), 1488–1511.
[12] R. Guo and T. Lin, A higher degree immersed finite element method based on a Cauchy extension for elliptic interface problems, *SIAM J. Numer. Anal.*, **57**:4 (2019), 1545–1573.
[13] Z.Q. Huang and E.J. Ding, *Transport Theory*, Science Press, 2008.
[14] A. Javili, S. Kaessmair, and P. Steinmann, General imperfect interfaces, *Comput. Methods Appl. Mech. Engrg.*, **275** (2014), 76–97.
[15] H. Ji, Q. Zhang, Q. Wang, and Y. Xie, A partially penalised immersed finite element method for elliptic interface problems with non-homogeneous jump conditions, *East Asian J. Appl. Math.*, **8** (2018), 1–23.
[16] D. Jia, Z. Sheng, and G. Yuan, An extremum-preserving iterative procedure for the imperfect interface problem, *Commun. Comput. Phys*, **25** (2019), 853–870.
[17] G. Jo and D.Y. Kwak, Enriched P_1-conforming methods for elliptic interface problems with implicit jump conditions, *Adv. Math. Phys.*, **2018** (2018): 9891281.
[18] D.Y. Kwak, S. Lee, and Y. Hyon, A new finite element for interface problems having Robin type jump, *Int. J. Numer. Anal. Model.*, **14**:4-5, (2017), 532–549.
[19] R.J. LeVeque and Z.L. Lin, The immersed interface method for elliptic equations with discontinuous coefficients and singular sources, *SIAM J. Numer. Anal.*, **31** (1994), 1019–1044.
[20] J. Li, J.M. Melenk, B. Wohlmuth, and J. Zou, Optimal a priori estimates for higher order finite elements for elliptic interface problems, *Appl. Numer. Math.*, **60** (2010), 19–37.
[21] Z. Li, H. Ji, and X. Chen, Accurate solution and gradient computation for elliptic interface problems with variable coefficients, *SIAM J. Numer. Anal.*, **55**:2 (2017), 570–597.
[22] T. Lin, D. Sheen, and X. Zhang, A nonconforming immersed finite element method for elliptic interface problems, *J. Sci. Comput.*, **79**:1 (2019), 442–463.
[23] K. Liu and Q. Zou, Analysis of a special immersed finite volume method for elliptic interface problems, *Int. J. Numer. Anal. Model.*, **16**:6 (2019), 964–984.
[24] G. Lopez-Ruiz, J. Bravo-Castillero, R. Brenner, M.E. Cruz, R. Guinovart-Díaz, L.D. Pérez-Fernández, and R. Rodríguez-Ramos, Variational bounds in composites with nonuniform interfacial thermal resistance, *Appl. Math. Model.*, **39**:23 (2015), 7266–7276.
[25] C.F. Matt and M.E. Cruz, Application of a multiscale finite-element approach to calculate the effective conductivity of particulate media, *Comput. Appl. Math.*, **21**:2 (2002), 429–460.
[26] H.V.R. Mittal and R.K. Ray, Solving immersed interface problems using a new interfacial points-based finite difference approach, *SIAM J. Sci. Comput.*, **40**:3 (2018), A1860–A1883.
[27] S. Monsurro and C. Perugia, Homogenization and exact controllability for problems with imperfect interface, *Netw. Heterog. Media*, **14**:2, (2019), 411.
[28] K.W. Morton and D.F. Mayers, *Numerical Solution of Partial Differential Equations*, Cambridge University Press, 2005.
[29] M. Oevermann, C. Scharfenberg, and R. Klein, A sharp interface finite volume method for elliptic

equations on Cartesian grids, *J. Comput. Phys.*, **228** (2009), 5184–5206.

[30] J. Pratibha and K. Manoj, Mathematical model and computer simulation of three dimensional thin film elliptic interface problems, *Comput. Math. with Appl.*, **63** (2012), 25–35.

[31] B. Preskill and J.A. Sethian, Jump splicing schemes for elliptic interface problems and the incompressible Navier-Stokes equations, *arXiv:1612.09342*, 2016.

[32] R.P.A. Rocha and M.E. Cruz, Computation of the effective conductivity of unidirectional fibrous composites with an interfacial thermal resistance, *Numer. Heat Tr. A-Appl.*, **39**:2 (2001), 179–203.

[33] C.N. Tzou and S.N. Stechmann, Simple second-order finite differences for elliptic PDEs with discontinuous coefficients and interfaces, *Commun. Appl. Math. Comput. Sci.*, **14**:2 (2019), 121–147.

[34] L. Wang, S. Hou, and L. Shi, A simple FEM for solving two-dimensional diffusion equation with nonlinear interface jump conditions, *Comput. Model. Eng. Sci.*, **119**:1 (2019), 73–90.

[35] Q. Wang and Z. Zhang, A stabilized immersed finite volume element method for elliptic interface problems, *Appl. Numer. Math.*, **143** (2019), 75–87.

[36] J. Weisz, On an iterative method for the solution of discretized elliptic problems with imperfect contact condition, *J. Comput. Appl. Math.*, **72** (1996), 319–333.

[37] H. Wu and Y. Xiao, An unfitted *hp*-interface penalty finite element method for elliptic interface problems, *J. Comput. Math.*, **37**:3 (2019), 316–339.

[38] G. Yuan and Z. Sheng. Monotone finite volume schemes for diffusion equations on polygonal meshes, *J. Comput. Phys.*, **227** (2008), 6288–6312.

[39] X. Zheng and J. Lowengrub, An interface-fitted adaptive mesh method for elliptic problems and its application in free interface problems with surface tension, *Adv. Comput. Math.*, **42**:5 (2016), 1225–1257.

[40] L. Zhu, Z. Zhang, and Z. Li, The immersed finite volume element method for some interface problems with nonhomogeneous jump conditions, *Int. J. Numer. Anal. Model.*, **13**:3 (2016), 368–382.